



저작자표시-비영리-변경금지 2.0 대한민국

이용자는 아래의 조건을 따르는 경우에 한하여 자유롭게

- 이 저작물을 복제, 배포, 전송, 전시, 공연 및 방송할 수 있습니다.

다음과 같은 조건을 따라야 합니다:



저작자표시. 귀하는 원저작자를 표시하여야 합니다.



비영리. 귀하는 이 저작물을 영리 목적으로 이용할 수 없습니다.



변경금지. 귀하는 이 저작물을 개작, 변형 또는 가공할 수 없습니다.

- 귀하는, 이 저작물의 재이용이나 배포의 경우, 이 저작물에 적용된 이용허락조건을 명확하게 나타내어야 합니다.
- 저작권자로부터 별도의 허가를 받으면 이러한 조건들은 적용되지 않습니다.

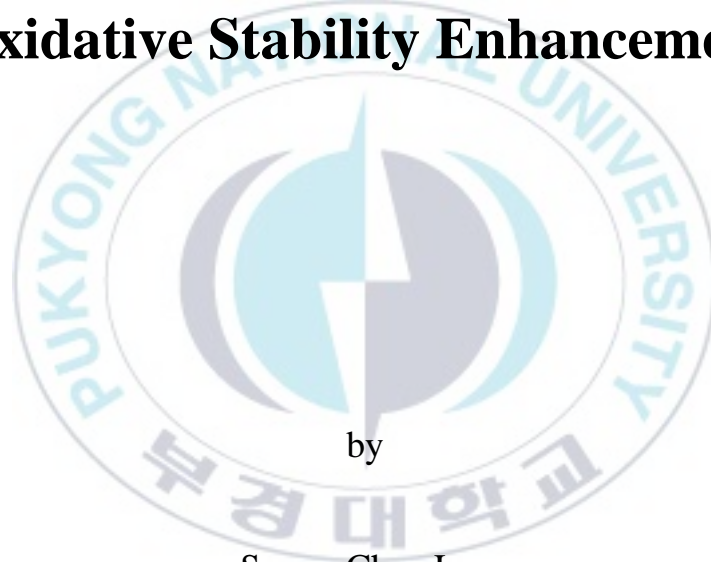
저작권법에 따른 이용자의 권리는 위의 내용에 의하여 영향을 받지 않습니다.

이것은 [이용허락규약\(Legal Code\)](#)을 이해하기 쉽게 요약한 것입니다.

[Disclaimer](#)

Thesis for The Degree of Master of Engineering

**Extraction and Encapsulation of
Squalene Rich Cod (*Gadus
macrocephalus*) Liver Oil Using
Supercritical CO₂ Processes for
Oxidative Stability Enhancement**



by

Seung-Chan Lee

Department of Food Science and Technology

The Graduate School

Pukyong National University

August, 2022

Extraction and Encapsulation of Squalene
Rich Cod (*Gadus macrocephalus*) Liver Oil
Using Supercritical CO₂ Processes for
Oxidative Stability Enhancement

초임계 이산화탄소 공정을 이용한 대구
(*Gadus macrocephalus*)
간으로부터 스쿠알렌이 함유된 오일의
추출 및 캡슐화를 통한 산화 안정성
증진

Advisor: Prof. Byung-Soo Chun

by

Seung-Chan Lee

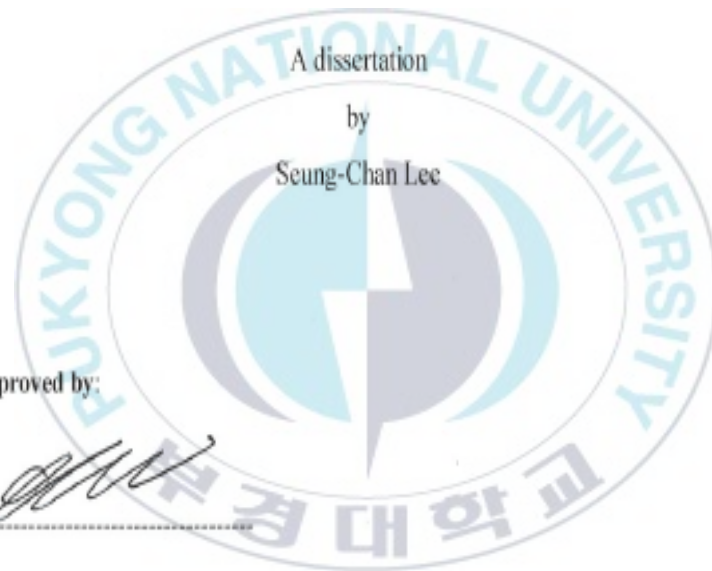
A thesis submitted in partial fulfillment of the requirements for the degree of

Master of Engineering

In Department of Food Science and Technology, The Graduate School,
Pukyong National University

August, 2022

Extraction and Encapsulation of Squalene Rich Cod (*Gadus macrocephalus*) Liver Oil Using Supercritical CO₂ Processes for Oxidative Stability Enhancement



A dissertation
by
Seung-Chan Lee

Approved by:

A handwritten signature in black ink, appearing to be "D. Ahn", written over a horizontal dashed line.

(Chairman)

Dong-Hyun Ahn, Ph.D.

A handwritten signature in black ink, appearing to be "K. Shim", written over a horizontal dashed line.

(Member)

Kil-Bo Shim, Ph.D.

A handwritten signature in black ink, appearing to be "B. Chun", written over a horizontal dashed line.

(Member)

Byung-Soo Chun, Ph.D.

2022 년 8 월 26 일

CONTENTS

List of Figures	iv
List of Tables	v
Abstract	vi
1. Introduction	1
1.1 <i>Gadus macrocephalus</i> and bioactive compounds.....	1
1.2 Supercritical carbon dioxide extraction.....	2
1.3 Particle production from gas saturated solutions.....	3
1.4 Objectives of the study.....	5
2. Materials and methods	6
2.1 Sample preparation.....	6
2.2 Chemical reagent.....	6
2.3 Oil extraction.....	7
2.3.1 Conventional extraction.....	7
2.3.2 SC-CO ₂ extraction.....	7
2.3.3 Experimental design for SC-CO ₂ extraction optimization.....	10
2.4 Proximate composition analysis of cod.....	13
2.5 Physicochemical analysis of cod liver oil.....	13
2.5.1 Color analysis.....	13
2.5.2 Chemical composition of cod liver oil.....	14
2.5.3 Heavy metal analysis.....	14

2.5.4 Thermogravimetric and FT-IR spectroscopic analyses.....	15
2.6 <i>In vitro</i> biological activities of the oil.....	17
2.6.1 Analysis of the antioxidant activity.....	17
2.6.2 Analysis of the antimicrobial activity.....	17
2.6.3 Cell culture and cell viability.....	18
2.7 Preparation of particles by PGSS process.....	19
2.8 Encapsulation efficiency (EE) by HPLC analysis.....	23
2.9 Particle characterization.....	24
2.9.1 Bulk, tapped density and compressibility index of the SLPs.....	24
2.9.2 Particle size analysis (PSA).....	24
2.9.3 Fourier transform infrared spectroscopy (FTIR).....	25
2.9.4 X-Ray Diffractometer (XRD).....	25
2.9.5 Scanning electron microscope (SEM).....	25
2.9.6 Differential scanning calorimeter (DSC).....	26
2.10 <i>In vitro</i> antioxidant activity assay.....	26
2.11 Acid value (AV) and peroxide value (POV).....	27
2.12 Statistical analysis.....	28
3. Results and discussion.....	30
3.1 Proximate composition analysis.....	30
3.2 Characterization and extraction optimization of cod liver oil.....	30
3.3 Thermal properties and FT-IR spectroscopy.....	41
3.4 Effect of the extraction technique on the bioactive compounds of cod liver oil...	45

3.5 Heavy metal composition.....	45
3.6 <i>In vitro</i> biological activities of the oils.....	49
3.7 Encapsulation yield and efficiency (EE).....	53
3.8 Bulk density and tapped density of SLPs and particle size analysis.....	56
3.9 Morphologies of SLPs.....	59
3.10 Fourier transform infrared spectroscopy (FTIR).....	61
3.11 X-Ray Diffractometer (XRD) and Differential scanning calorimeter (DSC).....	63
3.12 Antioxidant activity.....	68
3.13 AV and POV value of SLPs.....	70
4. Conclusions.....	72
References.....	74
Abstract (in Korean).....	84
Acknowledgement.....	87

List of Figures

- Fig. 1.** Schematic diagram of supercritical carbon dioxide extraction
- Fig. 2.** Schematic diagram of laboratory scale PGSS process system
- Fig. 3.** Extracted oils from different techniques (a) cold pressed cod liver oil; CCO, (b) hexane extracted cod liver oil; HCO, (c) SC-CO₂ extracted cod liver oil; SCO
- Fig. 4.** Three-dimensional response surface plot and contour plot representing effects: (A) Temperature (B) Pressure (C) Flow rate and SC-CO₂ extracted oil yield curve in time interval
- Fig. 5.** Thermal properties of the oils obtained from different extraction techniques: (a) Thermogravimetric analysis (TGA), (b) Derivative thermalgravimetric analysis (DTG) and Infrared absorption properties of squalene and oils by FT-IR analysis (c)
- Fig. 6.** Heavy metal composition of cod liver sample and oils from different extraction techniques (a) Mercury (Hg), (b) Arsenic (As), (c) Cadmium (Cd). Different letters indicate significant difference ($p < 0.05$)
- Fig. 7.** In-vitro biological activities of oils for antioxidant and cell viability assays (a) DPPH, (b) ABTS⁺, (c) FRAP, (d) AGS cell viability
- Fig. 8.** Squalene contents and encapsulation efficiency chromatogram by HPLC analysis standard; SCO; 3-PEG, 6-PEG; 9-PEG
- Fig. 9.** SEM micro graphs of SLPs recovered from different conditions at magnifications of $\times 150$ (a) 3-PEG, (b) 6-PEG, (c) 9-PEG
- Fig. 10.** Fourier transform infrared spectra for squalene, SCO, PEG and SLPs recovered from different conditions (i.e., \circ and \bullet for SCO and PEG, respectively)
- Fig. 11.** X-ray diffraction patterns of PEG and SLPs recovered from different conditions
- Fig. 12.** DSC endothermic and exothermic chromatogram of SCO, PEG and SLPs
- Fig. 13.** Antioxidant activity evaluation of SCO and SLPs (a) ABTS⁺, (b) DPPH
- Fig. 14.** AV and POV value of SCO and 9-PEG changes on days (a) acid value (b) peroxide value

List of Tables

- Table 1.** Box-Behnken experimental design for the response (the oil yield) from 17 runs combining different independent parameters for Temperature (A), pressure (B) and CO₂ flow rate (C)
- Table 2.** High performance liquid chromatography (HPLC) operating conditions used for detecting different functional compounds in cod liver oils
- Table 3.** The operating conditions for recover the SCO encapsulated SLP
- Table 4.** Proximate compositions of freeze-dried cod liver
- Table 5.** Color properties of cod liver oils obtained by different techniques
- Table 6.** Analysis of Variance (ANOVA) of the model response fitting parameters, and regression coefficients
- Table 7.** Oil extraction yield by using conventional techniques
- Table 8.** HPLC and GC results from the analysis of vitamins, squalene and omega-3 PUFAs
- Table 9.** Minimum inhibitory concentration (MIC) and minimum bactericidal concentration (MBC) of cod liver oil against *E. coli* and *B. cereus*
- Table 10.** Recovered SLPs yield and squalene encapsulation efficiency on different pressure and mixing ratio conditions
- Table 11.** Recovered SLPs density and particle size on different pressure and mixing ratio conditions
- Table 12.** Recovered SLPs, PEG and SCO crystallization temperature and melting point from DSC analysis

Extraction and Encapsulation of Squalene Rich Cod (*Gadus macrocephalus*)
Liver Oil Using Supercritical CO₂ Processes for Oxidative Stability
Enhancement

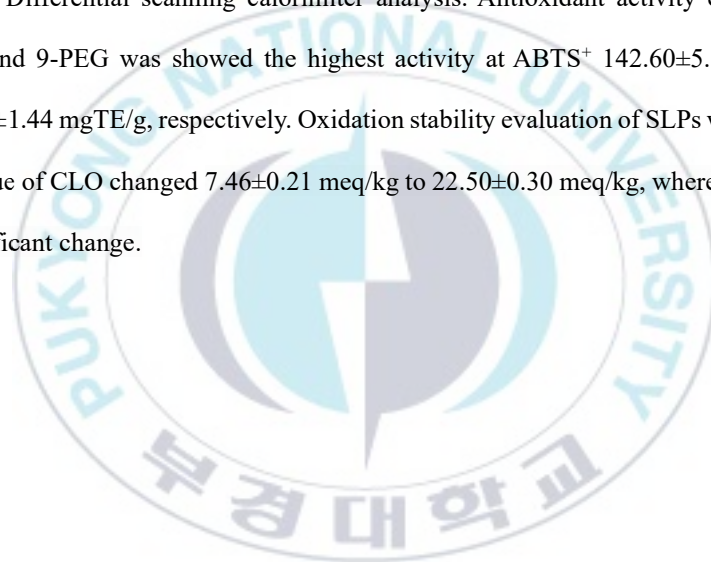
Seung-Chan Lee

Department of Food Science and Technology, The Graduate School,
Pukyong National University

Abstract

Cod liver oil (CLO) was extracted using conventional hexane and pressing methods or ecofriendly supercritical carbon dioxide (SC-CO₂). The extraction main parameters including temperature (A), pressure (B), and CO₂ flow rate (C) were optimized using response surface methodology. The oil chemical composition, safety, thermostability, and biological properties were characterized. The optimized SC-CO₂ extraction conditions were A = 49°C, B = 29.9 MPa, and C = 4.97 mL/min. Time-dependent extraction curves revealed a 68%, 85%, and 89% CLO recovery in 5, 15, and 20 h, respectively. SC-CO₂-extracted oil contained the highest squalene ($\approx 150 \mu\text{g/mL}$) and vitamins D and K concentrations and the lowest toxic heavy metal levels. Thermogravimetric analysis indicated that SC-CO₂-extracted oil was more susceptible to thermal degradation because of its high purity. SC-CO₂-extracted CLO exhibited radical scavenging and antimicrobial functions and was cytotoxic for cancer cells suggesting its potential use in the nutraceutical industry and novel functional material designs. Solid-lipid particles (SLPs) were obtained using particle production from gas saturated solutions (PGSS) process, which is a clean process, with the wall matrix poly-ethylene glycol. The yield and

encapsulation efficiency were $71.13 \pm 0.44\%$, $35.52 \pm 0.22\%$, respectively under the conditions of 25 MPa, 4:20 (SCO:PEG, w/w); 9-PEG. Bulk density and tapped density were $0.30 \pm 0.02 \text{ g/cm}^3$, $0.33 \pm 0.02 \text{ g/cm}^3$, respectively, at the 9-PEG, and Carr's index value was 9.09 ± 0.97 . The particle size was 315.83 nm at 9-PEG, and the typical form of powder from PGSS process was confirmed through a scanning electron microscope. The presence of squalene in the CLO and the encapsulation of CLO in the SLPs were confirmed through fourier transform infrared spectroscopy analysis. The crystallinity of SLPs were confirmed using the X-Ray diffractometer analysis and Differential scanning calorimeter analysis. Antioxidant activity evaluation was performed, and 9-PEG was showed the highest activity at ABTS⁺ $142.60 \pm 5.71 \text{ mgTE/g}$, at DPPH $30.38 \pm 1.44 \text{ mgTE/g}$, respectively. Oxidation stability evaluation of SLPs was performed, peroxide value of CLO changed $7.46 \pm 0.21 \text{ meq/kg}$ to $22.50 \pm 0.30 \text{ meq/kg}$, whereas SLP did not show a significant change.



1. Introduction

1.1. *Gadus macrocephalus* and bioactive compounds

Cod (*Gadus macrocephalus*) is a widely consumed fish species worldwide and this production is increasing from 3,536 ton in 2015 to 4,823 tons in 2020, especially in South Korea. Cod liver constitutes an extensive part of visceral wastes. Cod liver oil is a well-known “nutraceutical” and is widely consumed, especially in Nordic countries, and cod liver oil contains abundant amounts of specific vitamins (A, D, E) and polyunsaturated fatty acids (PUFAs; eicosapentanoic acid, docosahexaenoic acid) and thus is used as a health supplement (Mondello, 2006). Moreover, cod liver oil contains a large amount of vitamin K and squalene (Gershbein, 1969). Exploiting cod liver as a source of functional ingredients including squalene constitutes a significant economic opportunity and is a great approach to fishery resource valorization and conversion into valuable ingredients (Caruso, Floris, Serangeli, & Di Paola, 2020). Squalene is a biologically active component extracted from shark liver. It is a natural lipid belonging to the triterpene hydrocarbon group (2,6,10,15,19,23-hexamethyltetracosane-2,6,10,14,18,22-hexane) with a symmetrical 30-carbon polyprenyl chemical structure (Gopakumar & Thankappan, 1986). Squalene's functional properties include radical scavenging activity. Specifically, squalene prevents lipid oxidation by scavenging singlet oxygen, which is an oxidation initiator. Previous studies have provided experimental *in vivo* and *in-vitro* evidence strongly endorsing squalene antioxidant properties (Senthilkumar, Yogeeta, Subashini, & Devaki, 2006). Additionally, squalene presents antibacterial and antifungal properties (Lippi, Targher, & Franchini, 2010).

Moreover, recent studies support an anticancer role of squalene, which is used as a primary nutritional supplement for preventing or alleviating the severity of certain types of cancer (Dormont, Brusini, Cailleau, Reynaud, Peramo, Gendron, et al., 2020). Squalene significantly improves the immune response against different disorders, such as malaria, tuberculosis, leishmaniasis, and meningitis (Macdonald & Soll, 2020).

1.2. Supercritical carbon dioxide extraction (SC-CO₂)

Different extraction techniques are employed to recover healthy lipids from marine resources. These include conventional extraction methods such as manual pressing or solvent, usually hexane, extraction. These methods present several disadvantages. Manual pressing results in low yield and recovery of crude oils containing unwanted materials, such as heavy metals and organic matters. Solvent extraction is associated with the accumulation and disposal of toxic and flammable solvents posing serious environmental and safety concerns. These conventional methods require additional costly processing steps to separate the oils from contaminants and solvents, exposing the oil to harsh processing affecting its quality, and to oxygen species responsible for oxidative degradation (Franklin, Haq, Roy, Park, & Chun, 2020).

Alternative green extraction techniques are becoming more attractive to the extraction and resource valorization industry due to the global concern over environmental pollution caused in part by toxic solvent disposal. Moreover, some green solvents yield high-quality products in comparison with those obtained with conventional solvents, rendering their use for extraction crucial for consumer safety (Chemat, Abert-Vian,

Fabiano-Tixier, Strube, Uhlenbrock, Gunjevic, et al., 2019). Supercritical carbon dioxide (SC-CO₂) extraction is a green technique suitable for the extraction of non-polar compounds. Due to the low critical temperature required to reach CO₂ supercritical state ($T_c = 31^\circ\text{C}$), thermolabile bioactive ingredients are easily extracted without concern over degradation (Ahmadkelayeh & Hawboldt, 2020). The cleanliness of the SC-CO₂ extraction is due to the easy separation of CO₂ from the extracts achieved by changing the operating thermodynamic conditions resulting in clean and safe product use. In the present study, the SC-CO₂ extraction process was applied to recover lipids from the cod liver (SCO) containing squalene and vitamin D. The recovered oil demonstrated potential biological activities attractive for new product design in functional food development, nutraceuticals, and cosmetics.

1.3. Particle production from gas saturated solutions (PGSS)

Fish oil, including the cod liver oil, is very vulnerable to oxidation due to its high unsaturated degree. In addition, the oxidation of lipids is a major cause of deterioration of many fats and oils containing foods and is also an important quality standard in the food industry (Yang, 2000). Oxidation of lipids occurs from processing to storage of cooking oil and not only produces small molecule substances such as peroxide, aldehyde, ketone, and acid, but also reduces the nutritional quality of food, and these by-products can also be harmful to human health (Xu, 2016). The squalene contained in cod liver oil is a rather stable molecule, especially in the absence of the oxygen, and these squalene exhibit high antioxidant activity but may exhibit weak antioxidant

activity due to competitive oxidation with, lipids and substrates (Naziri, 2014). Since the oxidation process results in undesirable fishy smell, which degrades the overall quality of oil, fish oil used for constraints and food purposes should be produced, stored and packaged in an optimal state. The use of many nutritional and pharmaceutical compounds interested in biological availability or low safety of these compounds, and it is difficult to properly administer compounds that can maintain sufficiently high concentrations during the required working period (Fraile, 2013). Encapsulation has been used to solve these problems, encapsulation techniques have been mainly studied to overcome the poor biopharmaceutical properties of many compounds with high pharmacological activity, and micro and nano-encapsulation can provide useful means of improving physicochemical stability of bioactive molecules while improving drug absorption (São Pedro, 2016). In this study, for extraction and encapsulation of functional oil containing squalene extracted from cod liver, supercritical carbon dioxide (SC-CO₂) extraction and particle production from gas saturated solutions (PGSS) process were applied and were produced solid-lipid particles (SLPs). Polyethylene glycol (PEG) polymer was used as a matrix for loading functional oil, and the PEG plasticizers for food, because it have a wide range of molecular weights from 300 g/mol to 10000 g/mol (Šešlija, 2018), and its low melting point, low toxicity, drug compatibility and hydrophilic properties, so PEG is widely used for encapsulation of functional oils (Pestieau, 2015). The two main processes involved in preparing SLP are dissolution and solvent evaporation, and the PGSS process is a particle forming technique based on the interaction between supercritical carbon dioxide and low melting point polymers and fats, where components are dissolved in supercritical

carbon dioxide. In this process, carrier such as polymers are dissolved or dissolved together with suspended active drug components, and generally, carbon dioxide is dissolved in these compounds, which can reduce dissolution temperature and glass transition temperature and significantly reduce viscosity. When this gas-saturated melting extended to atmospheric pressure, the release of the dissolved gas causes a rapid temperature drop due to the Joule-Thomson effect and an increase in the melting temperature from ambient pressure to a typical value, both effects of which leads to very fast coagulation of polymers or oils. These resulting products are balanced with SC-CO₂ and expand through nozzle in the expansion chamber to form fine and porous composite particles (Fages, 2004, Griffin, 2014). The PGSS process has been used to process a wide range of food and pharmaceutical products, and based on previous experiments, it has been particularly successful in the formation of microcomposites or microcapsules of these compounds with lipid polymers as carrier (Varona, 2010).

1.4. Objectives of the study

In the literature review, there have been no studies about SC-CO₂ and the PGSS process of oil from cod (*Gadus macrocephalus*). Even though there are a lot of functional components such like vitamin A, D, E, K, omega-3 fatty acids and squalene. Therefore, in this experiment, functional oil extraction and powder production containing squalene for food and pharmaceutical applications was produced from cod liver, which a by-product, using the clean process SC-CO₂ extraction and PGSS process.

2. Materials and methods

2.1. Sample preparation

Cod livers were purchased from the Oepo port on Geoje island, the Republic of Korea. It was washed with tap-water and freeze-dried for 72 h by using a freeze dryer (HyperCOOL HC8080, BMS Co., Ltd., Republic of Korea) and stored at -70°C until their use for experiments.

2.2. Chemical reagents

CO_2 used for extraction and production of SLPs was purchased from KOSEM (Sahagu, Korea; 99.5% pure). The bacterial strains *Bacillus cereus* (Gram-positive) and *Escherichia coli* (Gram-negative) were obtained from the Korean Collection for Type Cultures and cultured in agar slant. AGS cell lines were bought from the American Type Culture Collection. PEG 8000 kDa was purchased from YAKURI PURE CHEMICALS (JAPAN). In addition, the solvents and reagents used in the experiment were used analytical or HPLC grade. Other solvents hexane (HPLC grade, 95%), methanol (HPLC grade, 99.9%), water (HPLC grade, 99.9%), acetonitrile (HPLC grade, 99.9%), Isopropyl alcohol (HPLC grade, 99.9%), Acetic acid (HPLC grade, 99.8%) were purchased from Samchun Chemical Co, Ltd, Republic of Korea. The standard of vitamin A, D₃,

K and squalene were purchased from Thermo Scientific, Rockford., IL. The other reagents and fatty acid (Supelco 37 Component FAME mix), 6-Hydroxy-2, 5, 7, 8-tetramethylchromane-2-carboxylic acid (Trolox, 97%), [2, 2-azinobis-(3-ethyl benzothiazoline-6-sulfonic acid)] (ABTS⁺), 2, 2-diphenyl-1-picrylhydrazyl (DPPH), [2, 4, 6-Tris(2-pyridyl)-s-triazine] (TPTZ), iron(iii) chloride were purchased from Sigma-Aldrich Chemical Co, USA. In addition, the solvents and reagents used in the experiment were used analytical or HPLC grade.

2.3. Oil extraction

2.3.1 Conventional extraction

CLO was extracted conventionally with hexane by mixing 100 g of the cod liver with 2 L of hexane. The mixture was stirred at 40°C for 24 h using a magnetic stirrer and was then filtered, the hexane was separated from the oil using a vacuum concentrator. The oil yield was expressed in percentage (%). For manual pressing extraction, 30 g of the cod liver was compressed using a manual compressor (Newtech, P00000GZ) and the quantity of oil recovered was expressed as % of yield.

2.3.2 SC-CO₂ extraction

SC-CO₂ extraction pressure, temperature, and CO₂ flow rate conditions were optimized using the response surface methodology (RSM) Box-Behnken Design

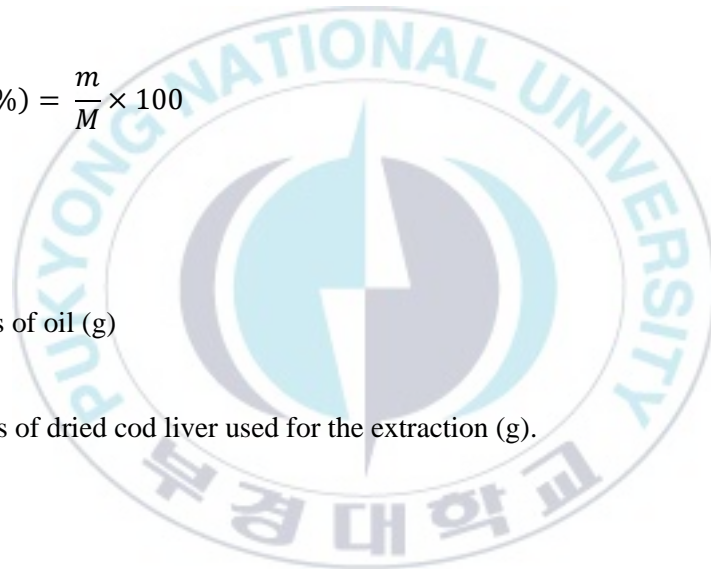
(BBD). The schematic diagram of the laboratory scale SC-CO₂ unit used for oil recovery is shown in Fig. 1 The system was equipped with a CO₂ supply tank, a chiller to condense the compressed CO₂ into liquid CO₂, heat exchangers to control the temperature of the extraction vessel and separator. The separator was equipped with a needle valve to control the CO₂ flow. A gas flow meter was used to measure the CO₂ consumption during the extraction process. The oil yield was expressed as the percentage of oil recovered following the equation (1).

$$\text{Oil yield (\%)} = \frac{m}{M} \times 100 \quad (1)$$

where

m : the mass of oil (g)

M : the mass of dried cod liver used for the extraction (g).



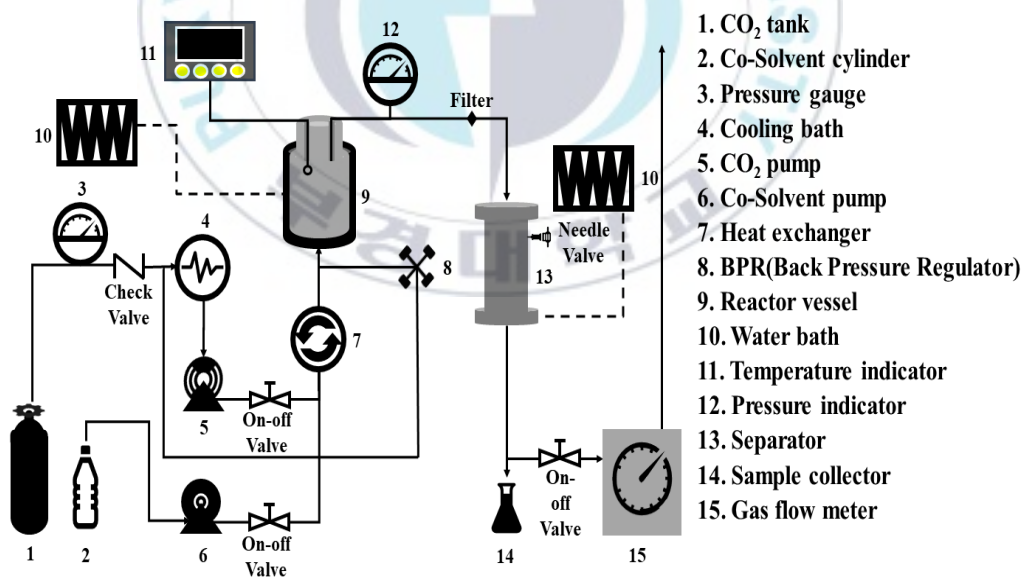


Fig. 1. Schematic diagram of supercritical carbon dioxide extraction

2.3.3 Experimental design for SC-CO₂ extraction optimization

The experiment was performed following the BBD to determine the interaction effects of the main process parameters, set as independent variables, driving the SC-CO₂ extraction. The temperature (A; °C), pressure (B; MPa), and CO₂ flow rate (C; mL/min) were selected as main factors influencing the SC-CO₂ extraction. The oil yield (y; %) was the response monitored to maximize the oil recovery from the cod liver. The levels of each parameter were set following previously published work on oil extraction from marine resources and preliminary screening experiments. Each coded variable ranged from -1 to +1 and the maximum and minimum ranges were set using the equation (2) commonly used for coding:

$$X = \frac{x - [x_{max} + x_{min}]/2}{[x_{max} - x_{min}]/2} \quad (2)$$

where

x : the natural variable

X : the coded variable

x_{max} : the maximum values for the natural variable

x_{min} : the minimum values for the natural variable.

Finally, independent variables, namely temperature, pressure, and CO₂ flow rate, which were factors influencing the extraction yield, ranged from the low level (-1) values of 40°C, 15 MPa, and 1 ml/min to high level (+1) values of 60°C, 30 MPa, and 5 mL/min, respectively.

A total of 17 runs was obtained from randomized combinations with 5 central repetitions. Their effects on the oil yield were assessed as shown in Table 1. The experimental results were fitted to the second-order polynomial model described in equation (3) to predict the different effects of the independent variables on the oil yield. Analysis of variance (ANOVA) was used to assess for the statistical significance, lack of fit, and regression coefficients for each term in the equation to verify the model.

$$Y = \beta_0 + \sum_{i=0}^3 \beta_i X_i + \sum_{i=0}^3 \beta_{ii} X_i^2 + \sum_{i < j}^3 \beta_{ij} X_i X_j \quad (3)$$

where

Y : represent the response variable

X_i : independent variables the response

X_j : independent variables affecting the response, and

β_0 : represents coefficients for intercept

β_i : represents coefficients for linear

β_{ii} : represents coefficients for quadratic

β_{ij} : represents coefficients for interaction terms.

Table 1. Box-Behnken experimental design for the response (the oil yield) from 17 runs combining different independent parameters for Temperature (A), pressure (B) and CO₂ flow rate (C)

Run	A (°C)	B (MPa)	C (mL/min)	Actual Yield (%)	Predicted Yield (%)
1	60	22.5	5.00	9.346	9.370
2	40	30.0	3.00	11.380	10.330
3	50	15.0	5.00	3.230	2.160
4	50	30.0	1.00	3.315	4.390
5	50	22.5	3.00	7.503	6.670
6	50	22.5	3.00	7.201	6.670
7	50	15.0	1.00	0.432	0.240
8	60	15.0	3.00	0.585	1.640
9	40	22.5	1.00	1.293	1.27
10	50	30.0	5.00	15.863	16.54
11	60	30.0	3.00	13.920	13.220
12	60	22.5	1.00	1.848	1.470
13	50	22.5	3.00	5.811	6.670
14	40	22.5	5.00	7.544	7.920
15	50	22.5	3.00	7.287	6.670
16	40	15.0	3.00	2.197	2.890

17	50	22.5	3.00	5.563	6.670
----	----	------	------	-------	-------

2.4 Proximate composition of cod liver

To analyze the oil proximate composition, crude lipids, crude proteins, ash, and moisture were measured according to the AOAC method (1997). The freeze-dried cod liver was dried at 105°C until constant weight and calculated the moisture content was determined. Also, crude protein was determined using Kjeldahl digester and measuring the nitrogen conversion factor (6.25) by multiplying. The crude lipid was determined using Soxhlet method, 5 g of freeze-dried cod liver was introduced in the thimble. Then, using 100 mL of n-hexane extract the lipid at 65°C for 16 h. After extract lipid, using a rotary evaporator remove the n-hexane at 50°C and calculated the mass of crude lipid. The ash content was determined by using calcination in a muffle furnace at 600°C for 10 h. The carbohydrate content was calculated by subtracting all proximate components from 100.

2.5 Physicochemical analysis of cod liver oil

2.5.1 Color

Calorimetric analysis was employed to assess the oil color with a Lovibond RT-series machine (The Tintometer Ltd, Amesbury, UK). The L^* (lightness), a^* (redness), and b^* (yellowness) values were expressed as three-dimensional values from the CIELAB color space. Standard plate values were $L^* = 95.08$, $a^* = -0.95$, and $b^* = 0.02$.

2.5.2 Chemical composition of cod liver oil

The CLO composition was analyzed as described previously (Bavisetty & Narayan, 2015) using an HPLC instrument (JASCO HPLC system, Tokyo, Japan) equipped with a UV-Vis detector and a Luna 5u C18 (2) 100A (4.6 × 250 mm) column. The injection volume was 10 μ l. Aliquots of the oil-chloroform mixture were syringe filtered before HPLC injection. The oil content in soluble vitamins A (retinol), D₃ (cholecalciferol), and K as well as squalene was analyzed. The description of the analytical methodology for each component, particularly the detection wavelength, oven temperature, mobile phase composition, and flow rate, are shown in Table 2. Each compound was quantified using the standard calibration curve of individual compounds.

The fatty acid analysis was conducted by using a GC-FID (Agilent Technologies, 7683B Series) equipped with a SUPELCO SPTM-2560 Fused Silica Capillary Column (100 m × 0.25 mm × 0.2 μ m) after the fatty acid methylation process following our previously described method (Nkurunziza, Ho, Protzman, Cho, Getachew, Lee, et al., 2021).

2.5.3 Heavy metal

The samples were pretreated in a carbolite furnace equipped with a heat controller for 12 h at 550°C. The ash was collected and dissolved in 10 mL of a 3% nitric acid solution. Then, it was filtered before the analysis of arsenic (As), cadmium (Cd), and lead (Pb) composition using an Inductively Coupled Plasma Mass Spectrometer (PERKIN ELMER NexION 300D). The mercury (Hg) content was measured using Automatic Mercury Analyzer (MILESTONE Tri-Cell DMA-80).

2.5.4 Thermogravimetric and FT-IR spectroscopy

The thermal stability was analyzed using a thermalgravimetric analyzer (TA Instruments Discovery DSC 25, Discovery TGA 55, TMA Q400). Briefly, 5 mg of oil were exposed to temperatures ranging from 50°C to 700°C with the temperature increasing at a rate of 10°C per min under N₂ gas to measure the oil weight loss and thermal stability. Derivative thermalgravimetric analysis (DTG) results were obtained by differentiating the TGA results. An FT-IR spectrometer (Jasco, Inc., USA) was used to obtain the IR spectrum recorded for wavelengths ranging from 650 to 4000 cm⁻¹.

Table 2. High performance liquid chromatography (HPLC) operating conditions used for detecting different functional compounds in cod liver oils

Parameters	Vitamin A	Vitamin D	Vitamin K	Squalene
Wavelength	325 nm	265 nm	250 nm	214 nm
Oven temperature	35 °C	40 °C	40 °C	40 °C
Mobile phase	MeOH:Water (90:10, v/v)	ACN:MeOH (90:10, v/v)	MeOH:IPA (90:10, v/v)	MeOH:IPA:Acetic acid (91.95:8:0.050, v/v)
Flow rate	1.0 mL/min	1.0 mL/min	1.0 mL/min	1.0 mL/min
Column	Luna 5u C18(2) 100A (4.6 × 250 mm)			
Injection volume	10 μ L			

2.6 *In vitro* biological activities of CLO

2.6.1 Antioxidant activity

The antioxidant activity of the CLO was analyzed using three antioxidant assays, namely the 2,2'-azino-bis (3-ethylbenzothiazoline-6-sulfonic acid (ABTS), 2,2-diphenyl-1-picryl-hydrazyl-hydrate (DPPH), and Ferric Reducing Antioxidant Power (FRAP) assays, following our previously published methods with minor modifications (Nkurunziza, Pendleton, Sivagnanam, Park, & Chun, 2019), (Bordoni, Fedeli, Nasuti, Maggi, Papa, Wabitsch, et al., 2019). Results were expressed in milligram Trolox equivalent per milliliter of oil (mgTE/mL, oil).

2.6.2 Antimicrobial activity

The minimum inhibitory concentration (MIC) and minimum bactericidal concentration (MBC) of CLO were evaluated with *Bacillus cereus* and *Escherichia coli* using the microdilution method. In brief, CLO was serially diluted at various concentrations (1000 to 1.95 µg/mL) in 10% dimethyl sulfoxide (DMSO) in a 96-well plate. Firstly, 100 µL of Mueller Hinton broth was added in up to 11 wells. Then, 100 µL of diluted CLO was added to the first well and mixed thoroughly. Afterward, 100 µL of the diluted sample was transferred into the next well and mixed thoroughly. This step was repeated up to the last well. After the oil gradual dilution, 5 µL of bacterial culture and 5 µL of resazurin were added to the wells in two different rows and mixed thoroughly. Then the plate was incubated at 37°C for 24 h. The procedure was applied

for the CCO, HCO, and SCO. The MIC was determined based on the color, ranging from blue to pink. To determine the MBC, 10 μL of the reaction mixture was transferred onto a sterile agar plate and incubated at 37°C for 24 h.

2.6.3 Cell culture and cell viability

To determine its toxicity for cells, the extracted oil was diluted in DMSO. Cells were cultured under the standard atmospheric condition with 5% CO_2 at 37°C and 95% humidity. The human gastric adenocarcinoma AGS cell line was cultured in Roswell Park Memorial Institute medium 1640 (RPMI 1640, GIBCO, Grand Island, New York, USA) supplemented with 10% heat-inactivated fetal bovine serum (Gibco, Grand Island, NY, USA), 100 U/mL penicillin, and 10 $\mu\text{g}/\text{mL}$ streptomycin (Hyclone, Logan UT, USA). AGS cells were cultured at 85% confluency until passage 4. Then, the cells were seeded in 96-well plates and allowed to attach. After 24 h, the medium was removed and the cells were treated with various concentrations of CLO extracted using different methods in a fresh medium for 24 h to check the anticancer activity. Afterward, the medium was replaced with a fresh RPMI medium. The cells were treated by adding 10 μL of EZ-Cytox (WST-1; Daeil Lab Service, Seoul, Republic of Korea) solution in each well following the manufacturer's instructions. The plates were incubated at 37°C for 2 h in the dark and then shaken for 5 s at medium speed on an ELISA microplate reader. The optical density at 460 nm was measured and used to quantify the viable cells. The viability of treated cells was plotted on a graph.

2.7 Preparation of particles by PGSS process

The schematic diagram of the laboratory scale PGSS unit used for producing the SLPs is shown in Fig. 2. Fig. 2 diagrammatically represents the PGSS unit used in this study. To obtain best highest encapsulation efficiency (EE%) of SCO using PGSS, we used different ratios of SCO, PEG and pressure (MPa) as follows Table 1. For each condition, the reaction mixer was loaded into the stainless-steel reactor chamber (200 mL) at a fixed reaction temperature of 50 C° using water bath (Water bath, Dong-won scientific., Co., Ltd, Seoul, Korea) with an agitation speed of 800 rpm for 1 h. CO₂ was pumped using high-pressure pump (SMN0000014, Hyosung., Co, Ltd, Seoul, Korea) into the reaction mixer via from a gas cylinder. The bottom of the mixing chamber as connected to the micronizer attached with a 400 μm capillary nozzle (60400, Ted Pella, Kanata, Canada) and the connected line was heated 60°C using heating cable (2359463129, Segicorp, Seoul, Korea) constant during 10 s depressurization. The final SLP microparticles were collected from the expansion chamber and the yield(%) was calculated using the following equation (4).

$$yield (\%) = \frac{m}{M} \times 100 \quad (4)$$

where

m : The mass of recovered powder in the expansion chamber (g).

M : The mass of initial SCO and PEG put in mixing chamber (g).



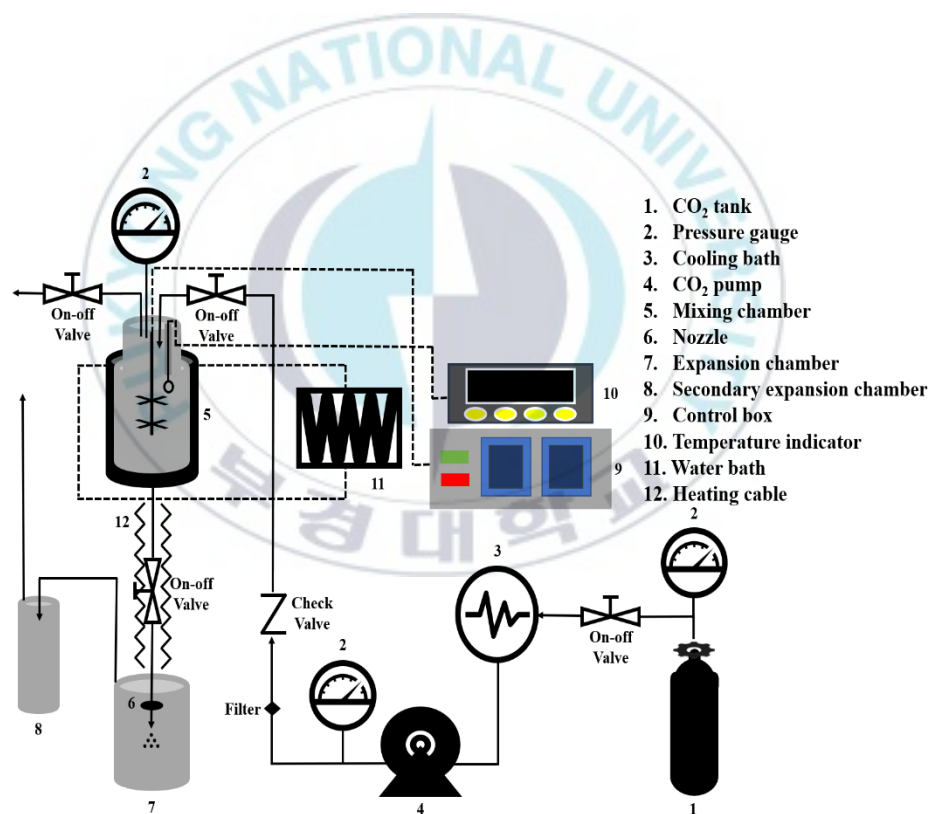


Fig. 2. Schematic diagram of laboratory scale PGSS process system

Table 3. The operating conditions for recover the SCO encapsulated SLP

Pressure (MPa)	Mixing ratio (SCO:PEG, w/w)	Nomenclature
15	1:20	1-PEG
	2:20	2-PEG
	4:20	3-PEG
20	1:20	4-PEG
	2:20	5-PEG
	4:20	6-PEG
25	1:20	7-PEG
	2:20	8-PEG
	4:20	9-PEG

2.8 Encapsulation efficiency (EE) by HPLC analysis

The squalene content in SCO and EE (%) were confirmed using an HPLC instrument (JASCO HPLC system, Tokyo, Japan) equipped with a UV-Vis detector. For the HPLC analysis, 1 mL of SCO was dissolved in 3 mL of chloroform, after filtered using a 0.45 μm hydrophobic filter, and then 10 μL injected. As for the pretreatment of SLPs, 1 g of SLPs were dissolved in 10 mL of water for melting PEG, then 2 mL of chloroform was added, and filtered after filtered using a 0.45 μm hydrophobic filter, then 10 μL injected. The corresponding analysis conditions for detecting squalene were wavelength: 214 nm, oven temperature: 40°C, mobile phase: MeOH: IPA: Acetic acid(91.95:8:0.05, v/v), flow rate: 1.0 mL/min. Through this analysis, the EE (%) of the squalene from SCO to SLPs encapsulated were calculated using equation (5) below.

$$EE (\%) = (Mp \times \frac{SQ_f}{SQ_i} / Mo) \times 100 \quad (5)$$

where

M_p : The mass of recovered SLP (g)

M_o : The mass of initial SCO (g)

SQ_i : The squalene content of the SCO ($\mu\text{g Squalene/g SCO}$)

SQ_f : The squalene content in the powder produced by PGSS process ($\mu\text{g Squalene/g SLP}$)

2.9 Particle characterization

2.9.1 Bulk, tapped density and compressibility index of the SLPs

The bulk density, tapped density and Carr's compressibility index (CI) of SLPs were carried out by slightly modified the method (Tun Norbrillinda, 2016). Briefly, 1 g of SLPs were added to 10 mL of an empty graduated cylinder, and the bulk density was calculated by dividing the mass (g) of the SLPs by the volume (mL) occupied by the SLPs. Tapped density were calculated by tapping the graduated cylinder 10 times at a height of 10 cm and dividing the mass (g) by the volume (mL) of the SLPs in the cylinder. From the results of bulk density and tapped density, the CI value were calculated following the equation (6).

$$CI = \frac{Td - Bd}{Td} \times 100 \quad (6)$$

where

Td : Tap density (g/cm³)

Bd : Bulk density (g/cm³)

2.9.2 Particle size analysis (PSA)

SLPs particle size analysis (PSA) measurement was performed by the edges light method using the Malvern Panalytical (Mastersizer 3000) size distribution equipment. After dissolving the SLPs powder in ethanol, the light diffraction wavelength of the microspheres in the suspension was measured. The size and degree of dispersion of the powder were identified from the measured wavelength, and the final particle size result was an average of the particle distribution of the sample represented by the volume surface diameters (d_{vs} , μm). The PSA comparison of SLPs obtained under different conditions was conducted in consideration of the cumulative distribution with a small particle size (D50) of 50 %.

2.9.3 Fourier transform infrared spectroscopy (FTIR)

Particles were analyzed at 649 and 4000 cm^{-1} using FTIR spectrometer (JASCO, FT-4100). Squalene and the SCO were measured, and the functional group of the SCO was identified to confirm the presence of squalene. For the comparison, the wall material PEG and PEG encapsulated SCO were analyzed to confirm whether the SCO was encapsulated well in PEG.

2.9.4 X-Ray Diffractometer (XRD)

The XRD analysis was performed using PANalytical (X'Pert3-Powder). The analysis conditions are generally taken from 5 to 35° on two θ scale, and the step size were 0.05° per s for qualitative analysis (Corrigan, 2002). A comparison with pure PEG was performed to confirm the crystallinity of the encapsulated SCO.

2.9.5 Scanning electron microscope (SEM)

The SEM measurement morphologies of the SLPs powder recovered using the PGSS process were obtained using JEOL, Gatan (JSM-6490LV, MonoCL3+). The morphology images were captured using the Sigma Scan Pro software (Systat Software Inc., CA, USA).

2.9.6 Differential scanning calorimeter (DSC)

Thermal energy flow analysis using DSC were performed using TA Instruments (Discovery DSC 25). The experiment was conducted as PEG, SLPs 6 mg, and SCO of 4 mg were weighed, then a continuous flow of N₂ gas was maintained through the heating cycle 10°C/min during 1.0 min then, heated from 10 to 150°C per 10°C/min and cooling cycle cooled to -60°C per 30°C/min.

2.10 *In vitro* antioxidant activity assay

Antioxidant activity of SCO and recovered SLPs were measured using ABTS⁺ and DPPH methods, and (Chamika, 2021) was used by modifying. Briefly, ABTS⁺ stock solution was prepared by mixing an equivalent amount of 7 mM ABTS⁺ and 2.45 mM

of potassium persulfate, then a dark reaction was performed at a room temperature during 16 h. 1 mL of ABTS⁺ stock solution was mixed with a 60 mL of MeOH solution, and the absorbance was measured at 734 nm, and the absorbance was adjusted to 0.7±0.02. ABTS⁺ assay, SCO was diluted with MeOH (1:3, v/v) and SLP with MeOH (1:3, g/v), then 100 µL of the supernatant mixed with 3.9 mL of ABTS⁺ solution, and a dark reaction was performed at a room temperature during 6 min. Afterwards, absorbance was measured at 734 nm. Likewise, the ABTS⁺, DPPH assay the 100 µL of the diluted solution were mixed with 0.2 mM DPPH ethanol solution of 3.9 mL, then performed a dark reaction at a room temperature for 30 min. Afterwards, absorbance was measured at 517 nm. Trolox was used as a standard material for comparison of antioxidant activity, and a calibration curve was prepared using a standard substance by concentration (1-1000 ppm), resulting milligram of Trolox equivalent per milliliter of oil and milligram of SLPs (mg TE/mL SCO, g SLP).

2.11 Acid value (AV) and peroxide value (POV)

Measurement of the acid value and peroxide value for checking the oxidation of encapsulated SLPs were determined according to the AOCS, (Xie, 2020). SCO and SLPs were stored at room temperature and the change of the acid value (AV) and peroxide value (POV) were measured per 3 days. Briefly, the AV measurement was performed by dissolving 1 g of SCO and 1 g of SLPs in 100 mL of ethanol:ether (1:2, v/v), and then using a 1% phenolphthalein solution as an indicator to be titrate as 0.1 N ethanolic potassium hydroxide. The calculation of AV was calculated using equation (7) and expressed as mg KOH/g.

$$\text{Acid value (mg KOH/g)} = \frac{(A-B) \times F \times 5.611}{W} \quad (7)$$

where

A : 0.1 N ethanolic potassium hydroxide volume used in sample titration (mL)

B : 0.1 N ethanolic potassium hydroxide volume used in blank titration (mL)

F : Titer of 0.1 N ethanolic potassium hydroxide

W : Weight of sample (g)

Briefly, the measurement of POV was performed by dissolving 1 g of SCO and 1 g of SLP in 25 mL of acetic acid:chloroform (3:2, v/v), adding 1 mL of saturated potassium iodine solution, and then reacted in a dark condition for 10 min. After the reaction, 30 mL of distilled water were added, and 1 mL of 1% starch solution was used as an indicator to be titrate for 0.01 N sodium thiosulfate solution. The calculation of POV was calculated using equation (8). and expressed as meq/kg.

$$\text{Peroxide value (meq/kg)} = \frac{(A-B) \times F \times 10}{W} \quad (8)$$

A : 0.01 N sodium thiosulfate volume used in sample titration (mL)

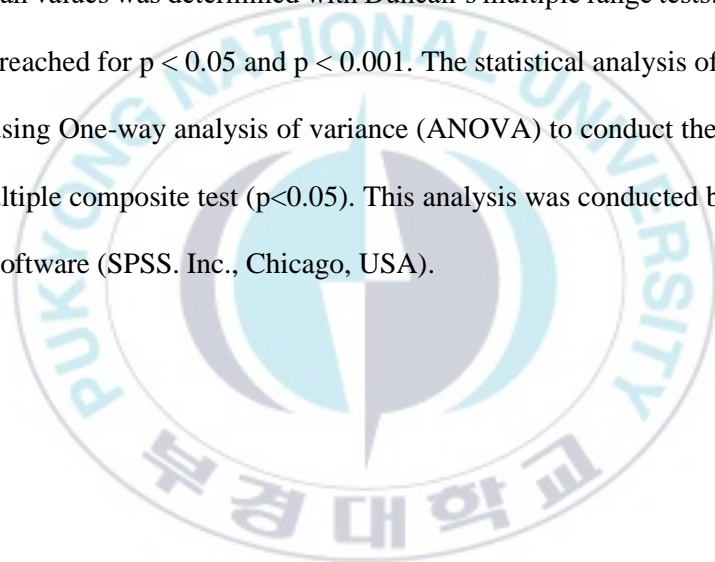
B : 0.01 N sodium thiosulfate volume used in blank titration (mL)

F : Titer of 0.01 N sodium thiosulfate

W : Weight of sample (g)

2.12 Statistical analyses

Each experiment was performed in triplicates and values were expressed as means \pm standard deviations. One-way ANOVA was performed using the SPSS software (version 20.0, SPSS Inc., Chicago, IL). The statistical significance of the difference from the mean values was determined with Duncan's multiple range tests. Significance levels were reached for $p < 0.05$ and $p < 0.001$. The statistical analysis of the data was conducted using One-way analysis of variance (ANOVA) to conduct the Tukey's and Duncan's multiple composite test ($p < 0.05$). This analysis was conducted by IBM SPSS version 27 software (SPSS, Inc., Chicago, USA).





3. Results and discussion

3.1 Proximate composition

The proximate composition of freeze-dried cod liver results is shown in the Table 3. The samples contained more than 50% of crude lipids ($56.62\% \pm 2.61\%$) and considerable levels of moisture ($21.58\% \pm 1.01\%$) and proteins ($12.91\% \pm 1.32\%$). The remaining trace components were attributed to the carbohydrates and ash content.

3.2 Characterization and extraction optimization of cod liver oil

Food color is an important sensory factor. The color of the oil is indicative of the potential presence of foreign substances that might interact with fatty acids and speed

up the oxidation process. Pictures of the oil obtained with the different extraction techniques are in Fig. 3 and the oil color properties are shown in Table 4. All color indicators were significantly different among the extraction technique applied. The lightness was greater in CCO and SCO with L^* values of 58.96 ± 0.72 and 48.39 ± 0.87 , respectively. The yellowness was dominant in SCO and CCO extracted oils, with b^* values of 29.36 ± 0.70 and 27.97 ± 0.79 , respectively. HCO resulted in a significantly darker color (Fig. 3c) with an L value of 32.96 ± 0.36 and the highest a^* value (9.60 ± 0.24) (Table 4). These results were anticipated since SC-CO₂ extraction is highly selective owing to the use of CO₂ as a non-polar solvent. Therefore, oil extracted with this technique contains fewer impurities and presents desirable yellowness and lightness characteristics. The darker color of oil extracted with hexane can be attributed to dissolved pigments and mixtures of both polar and non-polar substances. Moreover, solvent removal by vacuum distillation might initiate thermal-induced oil oxidation, which might affect the oil color.

The SC-CO₂ extraction was optimized for pressure, SCO₂ flow rate, and temperature, and their interactive influence on oil yield was assessed. A total of 17 runs were performed representing a combination of high, medium, and low levels in the range of the experimental domain. The parameter effects on the oil yield are shown in Table 1. The lowest and highest oil yields were approximately 0.43% and 15.86%, respectively, and were associated with the combined effects of pressure and CO₂ flow rate. Indeed, the lowest pressure (15 MPa) and CO₂ flow rate (1 mL/min) were correlated with the lowest oil yield in both the predicted and actual responses. In contrast, the highest pressure (30 MPa) and CO₂ flow rate (5 mL/min) were associated with the highest yield.

These observations agreed with previous studies, which reported the positive effects of increased pressure and CO₂ flow rate on oil recovery (Ruslan, Idham, Nian Yian, Ahmad Zaini, & Che Yunus, 2018).

To predict and verify the model, a multiple regression analysis was performed. The second-order polynomial equation (equation 4), which expresses the interactions of variables and their effect on the model predictability of the parameter effects on the process, was assessed by the coefficient of variation analysis. The statistical significance of the model, individual variables, and interactive variables was analyzed by ANOVA (Table 5).

$$\begin{aligned}
 Y = & 10.72047 - 0.13973A - 0.096550B - 0.38537C + 1.38400 \times 10^{-4}AB \\
 & + 155.87 \times 10^{-4}AC \\
 & + 162.250 \times 10^{-4}BC - 1.77375 \times 10^{-3}A^2 \\
 & + 9.33111 \times 10^{-5}B^2 \\
 & - 371.97 \times 10^{-3}C^2
 \end{aligned} \tag{9}$$

The model was highly significant ($p < 0.0002$), indicating that it can be used to predict the outcome of the experimental domain. The statistical analysis of the independent variables indicated that the temperature did not significantly ($p < 0.3641$) influence the extraction yield, whereas the pressure and CO₂ flow rate effects were highly significant ($p < 0.0001$).



Table 4. Proximate compositions of freeze-dried cod liver

Compositions	Raw material (%)
Crude protein	12.91±1.32
Crude lipid	56.62±2.61
Carbohydrate	7.58±2.22
Moisture	21.58±1.01

Ash

1.31±0.22

Mean ± SD (n=3).

Different letters indicate difference ($p < 0.05$) according to Duncan's multiple range test.

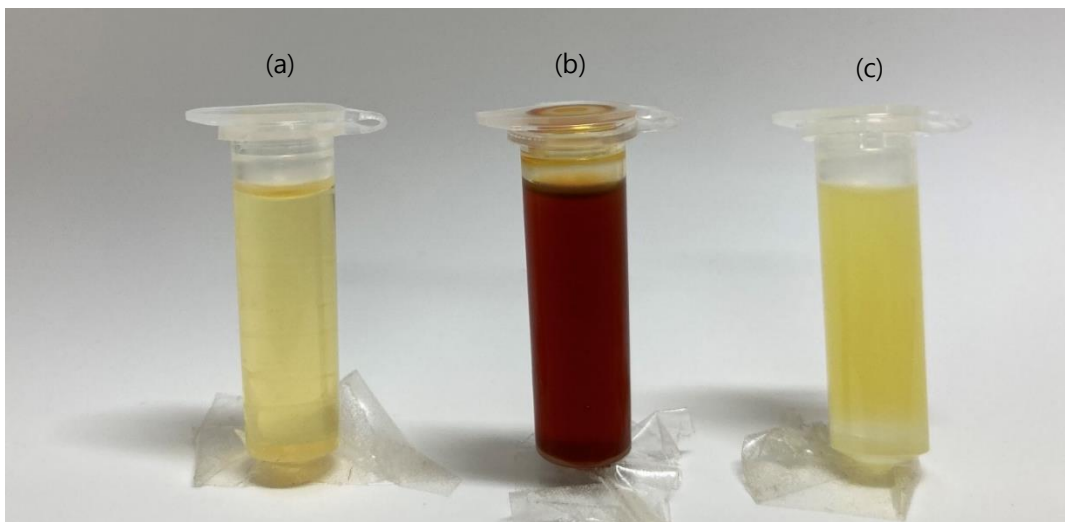


Fig. 3. Extracted oils from different techniques (a) cold pressed cod liver oil; CCO, (b) hexane extracted cod liver oil; HCO, (c) SC-CO₂ extracted cod liver oil; SCO



Table 5. Color properties of cod liver oils obtained by different techniques

Mean \pm SD (n=3),

Different letters indicate difference ($p < 0.05$) according to Duncan's multiple range test.

Conditions	L*	a*	b*
CCO	58.96 \pm 0.72 ^a	-4.53 \pm 0.10 ^c	27.97 \pm 0.79 ^b
HCO	32.96 \pm 0.36 ^c	9.60 \pm 0.24 ^a	5.31 \pm 0.19 ^c
SCO	48.39 \pm 0.87 ^b	8.70 \pm 0.21 ^b	29.36 \pm 0.70 ^a

Table 6. Analysis of variance (ANOVA) of the model response fitting parameters, and regression coefficients

Source	Sum of Squares	df	Mean Square	F Value	p-value Prob > F	
Model	326.84	9	36.32	25.36	0.0002	significant

A-Temperature	1.35	1	1.35	0.94	0.3641	
B-Pressure	180.82	1	180.82	126.29	< 0.0001	
C-Flow rate	105.81	1	105.81	73.91	< 0.0001	
AB	4.31	1	4.31	3.01	0.1263	
AC	0.39	1	0.39	0.27	0.6184	
BC	23.77	1	23.77	16.60	0.0047	
AA	0.13	1	0.13	0.093	0.7698	
BB	1.16	1	1.16	0.81	0.3980	
CC	9.32	1	9.32	6.51	0.0380	
Residual	10.02	7	1.43			
Lack of Fit	6.70	3	2.23	2.69	0.1814	not significant
Pure Error	3.32	4	0.83			
Cor Total	336.86	16				

R-squared = 0.9702; Adj R-squared = 0.9320; Pred R-squared = 0.6662; Adeq precision (signal to noise ratio) = 18.287.

This observation was consistent with previous studies, in which the temperature had minor effects on the oil yield during SC-CO₂ extraction (Confortin, Toderò, Soares, Brun, Luft, Ugalde, et al., 2017). Increasing the temperature under isobaric conditions might lower the solvation power of SC-CO₂ and reduce the extraction rate by decreasing the density of CO₂ (Yang, Wei, Huang, & Lee, 2013). The model indicated that the pressure and CO₂ flow rate interaction effect was significant ($p < 0.0047$). An increase in pressure during SC-CO₂ extraction increased the density, which enhanced

the solubility of the solute in SC-CO₂. An increase in the CO₂ flow rate improves the mass transfer properties and extraction yield (Ndayishimiye, Getachew, & Chun, 2017). Further verification of the model accuracy showed an insignificant lack of fit together with the coefficients of variations, $R^2 = 0.9702$, adjusted $R^2 = 0.932$, and predicted $R^2 = 0.666$, supporting the model accuracy. Therefore, the model equation can be used for interpolation in the experimental domain as it defined the true behavior of the system.

To further validate the model, three-dimensional contour plots were generated to illustrate the interaction effects of independent variables on the response (Fig. 4 a,b,c). The analysis of pressure vs. temperature interactions revealed that the response (% yield) was affected by variations of pressure, whereas varying temperature did not affect the yield (Fig. 4a). A similar trend was confirmed when analyzing the interaction effects of flow rate vs. temperature, the response was highly dependent on the CO₂ flow rate and not on the temperature (Fig. 4b). However, the analysis of the interaction of flow rate vs. pressure indicated that increasing both parameters affected the oil yield (Fig. 4c). Overall, our results showed that the pressure and CO₂ flow rate are the influential parameters for maximizing the extraction of oil from the cod liver. The exact optimum extraction conditions were a temperature of 49°C, a pressure of 29.9 MPa, and a CO₂ flow rate of 4.97 mL/min. Under the optimum conditions of pressure, CO₂ flow rate, and temperature, the overall yield of CLO achieved with SC-CO₂ extraction was determined by plotting an extraction curve of oil yield against the extraction time (Fig. 4d). The oil yield increased exponentially within 5 h of extraction reaching nearly 38%. The extraction yield continued to increase with the extraction time at a slower rate until 15 h of extraction time to $\approx 48\%$. After this period, the increase in oil yield

was trivial as the oil recovery reached a plateau. The overall SC-CO₂-extracted oil yield after 20 h was around 50% (Fig. 4d). In comparison with other extraction techniques, manual pressing (CCO), and hexane extraction (HCO) yielded 31.32 ± 4.61 and 55.72 ± 2.61 respectively (Table 6).



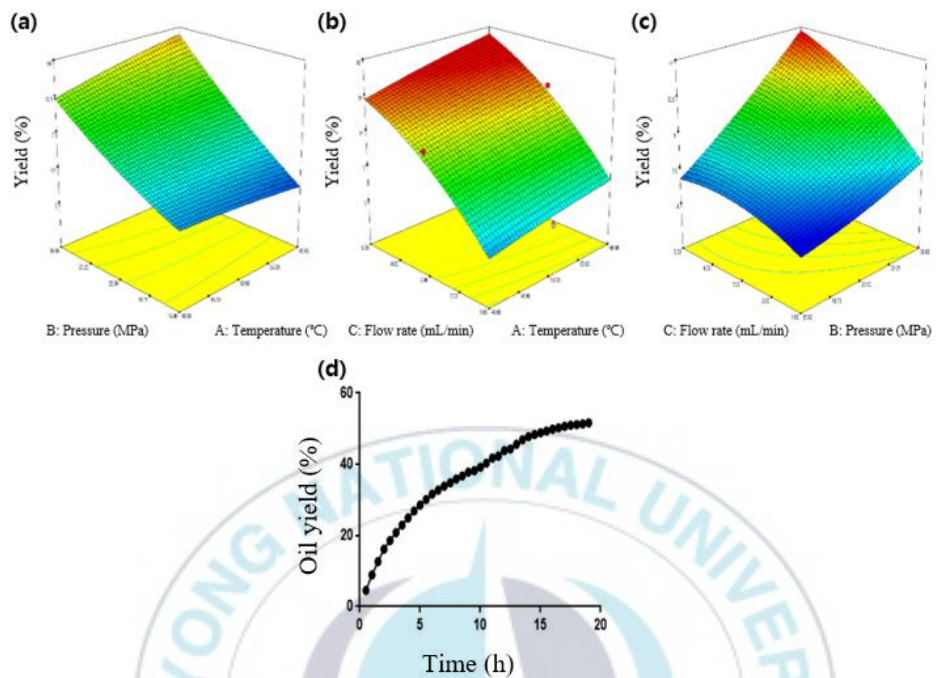


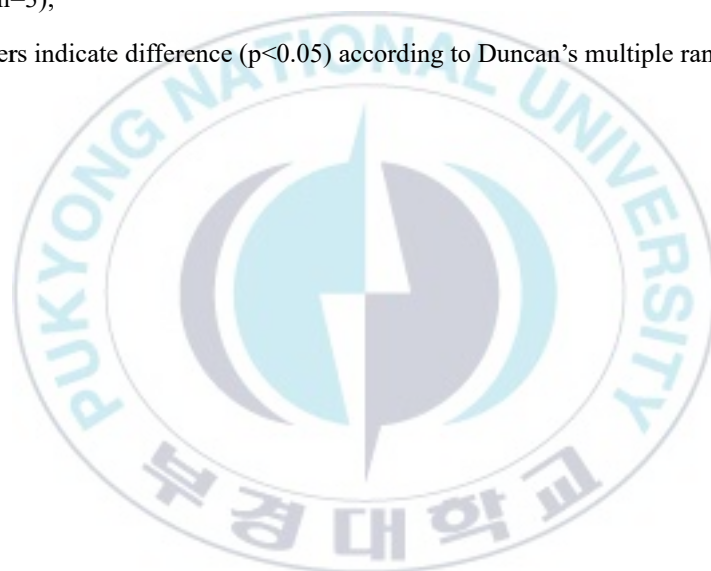
Fig. 4. Three-dimensional response surface plot and contour plot representing effects: (A) Temperature (B) Pressure (C) Flow rate and SC-CO₂ extracted oil yield curve in time interval

Table 7. Oil extraction yield by using conventional techniques

Extraction method	CCO	HCO
Oil yield (%)	31.32±4.61 ^b	55.72±2.61 ^a

Mean ± SD (n=3),

Different letters indicate difference ($p < 0.05$) according to Duncan's multiple range test.



3.3 Thermal properties and FT-IR spectroscopy

The TG and DTG curves showed the thermal decomposition profile of CLO obtained with different extraction techniques (Fig. 5a, b). The SCO and HCO weight loss decreased substantially with increasing temperatures between 190°C and 270°C, with

weight losses of approximately 24% for SCO and 16% for HCO. However, under similar temperature conditions, only 4% of CCO weight loss was observed. It was noticed that at a temperature of 300°C, the rate of decomposition remained faster for SCO with mass loss of approximately 27%, whereas the 18% weight loss was observed for HCO. Surprisingly, the decomposition rate for temperatures up to 330°C was remarkably slower for CCO with a weight loss of only 7% as shown by the TG curves (Fig. 5a). For temperatures above 330°C, a dramatic weight loss affected all oil samples regardless of the extraction technique and all samples were fully degraded at 470°C. The decomposition profile of CLO showed differences in the oil chemical composition depending on the extraction technique. The fastest decomposition rate seen in SCO might be attributed to the purity of the oil recovered by SC-CO₂ extraction using the non-polar solvent CO₂, which selectively dissolve non-polar lipids. Moreover, SC-CO₂ extraction is performed under a closed system preventing the adsorption of oxygen by fatty acid chains. This is advantageous because the formation of peroxides in SC-CO₂-extracted oils is avoided. In contrast, both hexane and cold press extractions expose the oil to oxygen leading to the accumulation of peroxide radicals. In terms of thermal decomposition, the accumulation of oxygen species might result in the slow decomposition seen for hexane-extracted and cold-pressed oils. Besides, the latter techniques, are not selective and the extracted crude oils might contain a wide range of impurities including phospholipids, complex metals, complex minerals, free fatty acids, and other polar compounds. S Sathivel *et al.* compared the thermal stability of catfish and menhaden oils at different refining steps and reported that the oil thermal stability decreased after each refining step (crude oil > degummed oil > neutralized oil >

bleached oil > deodorized oil) (Sathivel, Prinyawiwatkul, Negulescu, King, & Basnayake, 2003). The presence of impurities has been associated with reduced effectiveness of heat transfer and resulted in less energy available to evaporate the volatiles (Huang & Sathivel, 2008), (Wesołowski & Erecińska, 1998). Therefore, SCO might possess fewer impurities, hence the lower value of the initial temperature of decomposition.

The FT-IR spectra of the extracted oils and squalene standard were recorded at mid-infrared regions ($4000\text{--}650\text{ cm}^{-1}$), and results are shown in Fig. 5c. Squalene exhibits antisymmetric stretching vibrations of -CH_3 , -CH_2 at 2968.87 and 2920.66 cm^{-1} , respectively, and asymmetric -CH_2 stretching vibration at 2857.99 cm^{-1} (Petrick & Dubowski, 2009). These absorption bands were detected in all oils with a stronger intensity for both methylene (-CH_2) groups, most likely because of these groups' presence in a wide variety of fatty acids. The absorption band at 1666.19 cm^{-1} for squalene was associated with a weak -C=C- stretching vibration. The vibration band in the CLO observed at 1742 cm^{-1} was associated with a -C=O stretching vibration of the carbonyl groups (carboxylic acid end groups) of different fatty acids in the extracted oils. In the fingerprint region, squalene vibration bands at 1445.4 and 1381 cm^{-1} are associated with the -CH_2 scissor and $\text{-C(CH}_3\text{)}$ symmetric bends (Petrick & Dubowski, 2009), which were also detected in the extracted CLOs, albeit at weak intensities, confirming the presence of squalene (Fig. 5c).



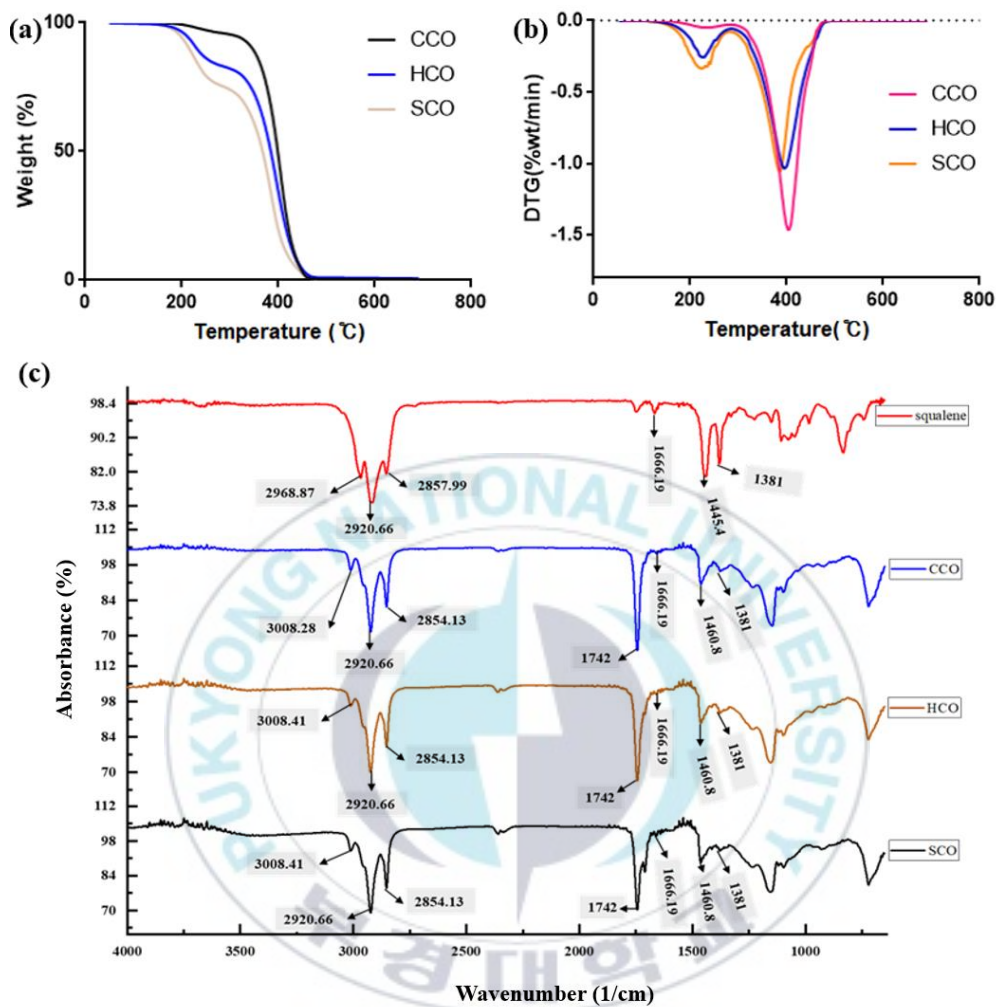


Fig. 5. Thermal properties of the oils obtained from different extraction techniques: (a) Thermogravimetric analysis (TGA), (b) Derivative thermalgravimetric analysis (DTG) and Infrared absorption properties of squalene and oils by FT-IR analysis (c)

3.4 Effect of the extraction technique on the bioactive compounds of

cod liver oil

Table 7 shows the concentration of different bioactive ingredients obtained from CLO including vitamins (A, D, and K), squalene, and omega-3 PUFAs. Vitamin A concentration was remarkably high in CCO (43.90 $\mu\text{g/mL}$), significantly higher than that of SCO. Hexane was inefficient at recovering vitamin A. On the other hand, the amount of vitamin D recovered in SCO (30.03 $\mu\text{g/mL}$) was two and six folds that recovered in HCO and CCO, respectively. Vitamin K, specifically K2 and K3, and squalene were remarkably more abundant in SCO than in oil obtained with other extraction techniques (Table 7). SC-CO₂ selectivity and ability to dissolve lipid-soluble vitamins and squalene imply its potential as an extraction method to recover functional oils. The poor solubility of vitamin A in SC-CO₂ might be improved by using a co-solvent. However, this is beyond the scope of this manuscript. It was also observed that CLO contained a remarkable amount of ω -3 PUFAs such as EPA and DHA known to exhibit numerous functional properties in humans.

3.5 Heavy metal composition

Toxic heavy metals pose a serious threat to the human body as they cause acute and chronic toxicities. They can lead to neurotoxicity and generate free radicals responsible for promoting oxidative stress and damages to proteins, lipids, and DNA molecules even in minimal amounts (Engwa, Ferdinand, Nwalo, & Unachukwu, 2019). Fig. 6 shows the concentration of heavy metals in the original freeze-dried cod liver samples and the extracted oils. The Hg and Cd content of the raw materials was significantly higher ($p < 0.05$) than the amounts found in the oil after extraction (Fig. 6a, c). However,

CCO presented a higher concentration of As than the raw material, HCO, or SCO (Fig. 6b). SC-CO₂ extraction generated the lowest concentration of any heavy metal analyzed compared with the other extraction systems. This might be attributed to the selectivity of SC-CO₂ extraction for non-polar compounds (Fig. 6). In agreement with our findings, the supercritical extraction of oils from fish processing byproducts was shown to significantly reduce the levels of toxic heavy metals to the recommended values (Rubio-Rodríguez, Sara, Beltrán, Jaime, Sanz, & Rovira, 2012). The significant reduction in the toxic heavy metals below their toxicity levels by SC-CO₂ extraction is a valuable advantage of using CO₂ as an extraction solvent. R. Ahmed et al. (Ahmed, Haq, Cho, & Chun, 2017) reported a significant reduction in the toxic heavy metal concentration after SC-CO₂ extraction of bigeye tuna byproducts to levels below the toxic concentration accepted by the FAO, whereas the levels obtained with hexane extraction were above the accepted limit. Pb was not detected in the raw material or extracted oils.

Table 8. HPLC and GC results from the analysis of vitamins, squalene and omega-3 PUFAs

Conditions	vitamins ($\mu\text{g/mL}$)				Squalene ($\mu\text{g/mL}$)	ω -3 PUFAs ($\mu\text{L/g}$)	
	Vit A	Vit D ₃	Vit K			EPA	DHA
			K ₂	K ₃			
CCO	43.90 \pm 0.99 ^a	6.42 \pm 0.04 ^c	2.12 \pm 0.14 ^b	36.64 \pm 0.45 ^c	15.63 \pm 0.90 ^c	17.50 \pm 0.24 ^a	32.53 \pm 0.38 ^a
HCO	1.68 \pm 0.03 ^c	15.53 \pm 0.26 ^b	2.09 \pm 0.24 ^b	63.18 \pm 0.53 ^b	120.90 \pm 4.55 ^b	14.32 \pm 0.61 ^b	28.85 \pm 1.46 ^b
SCO	6.11 \pm 0.17 ^b	30.03 \pm 0.85 ^a	2.90 \pm 0.19 ^a	112.63 \pm 0.54 ^a	149.31 \pm 9.99 ^a	13.91 \pm 0.43 ^b	23.41 \pm 0.96 ^c

Mean \pm SD (n=3),

Different letters indicate difference ($p < 0.05$) according to Duncan's multiple range test.

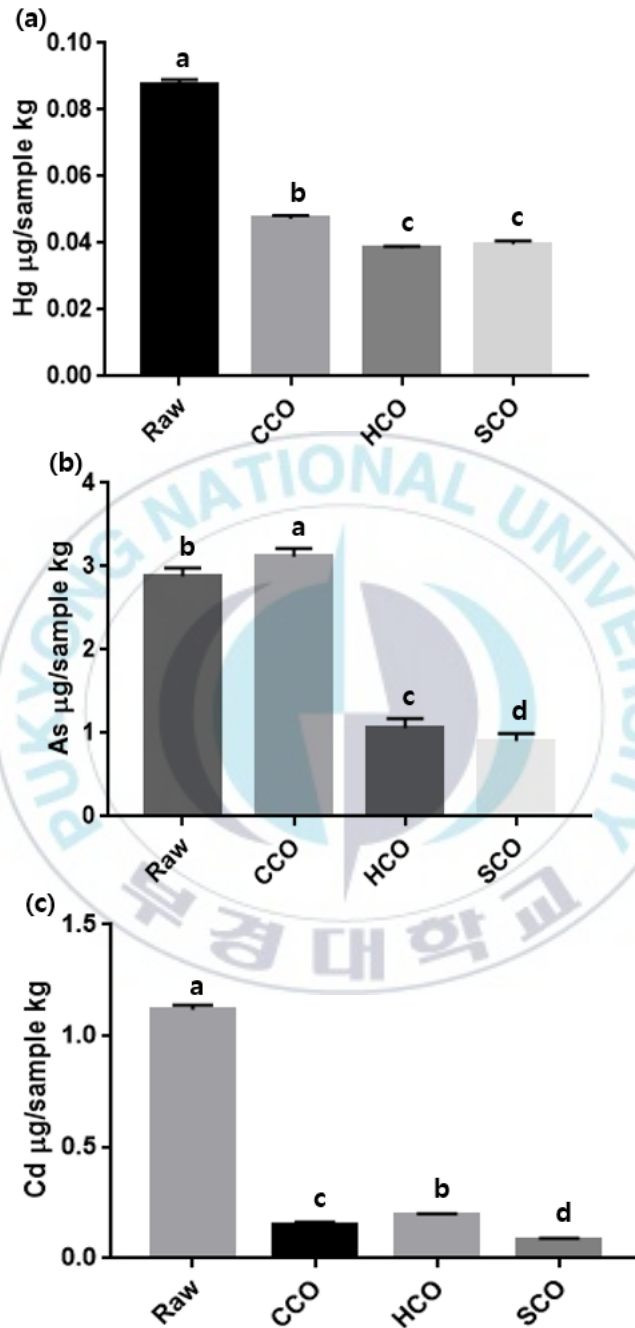
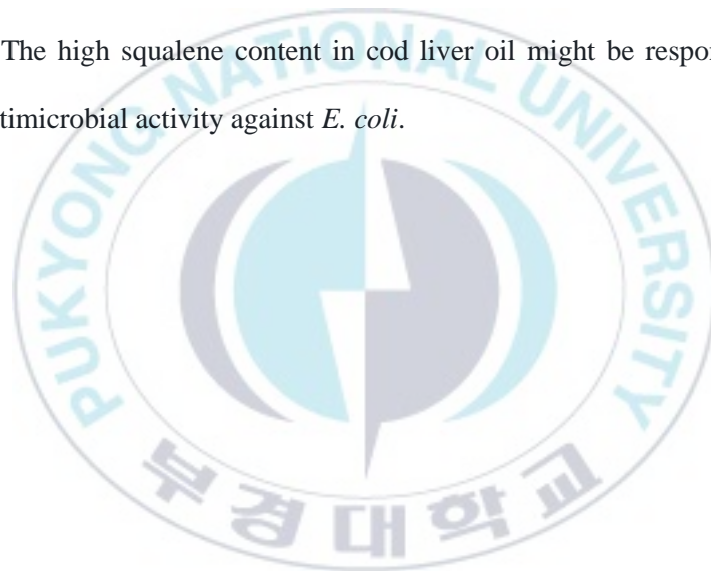


Fig. 6. Heavy metal composition of cod liver sample and oils from different extraction techniques (a) Mercury (Hg), (b) Arsenic (As), (c) Cadmium (Cd) Different letters indicate significant difference ($p < 0.05$)

3.6 *In vitro* biological activities of the oils

The antioxidant and cytotoxicity of CLOs were evaluated. The results are presented in Fig. 7. The oil antimicrobial activities are shown in Table 8. There were no differences between HCO and SCO radical scavenging and reducing power activities assessed by DPPH and FRAP assays (Fig. 7a and c). This might be attributed to the comparable concentration of squalene in the extracted oils (Table 7). Moreover, the amounts of squalene in CCO were nearly 10 and 8 times lower than the concentration in SCO and HCO, respectively (Table 7). Consequently, the antioxidant activities of CCO were significantly lower ($p < 0.05$) than that of HCO and SCO (Fig. 7). Squalene is a powerful natural antioxidant and higher squalene concentration in the oil has been associated with higher oil antioxidant activities (Kraujalis & Venskutonis, 2013). Squalene has demonstrated strong *in vivo* antioxidant activities in mice and was suggested to modulate oxidative stress and inflammatory responses (Kumar, Narayan, Sawada, Hosokawa, & Miyashita, 2016). The viability of a human gastric adenocarcinoma cell line (AGS cells) was tested to determine the anti-cancer properties of the oils (Fig. 7d). CCO exhibited a significantly lower potency against AGS with an IC_{50} value of approximately 800 $\mu\text{g/mL}$. The IC_{50} value decreased significantly after treating the cells with HCO ($\approx 600 \mu\text{g/mL}$), probably due to a higher amount of squalene, vitamin D, and vitamin K. AGS cells were highly susceptible to SC-CO₂ extracted oil (SCO) which exhibited a drastically lower IC_{50} value of 90 $\mu\text{g/mL}$, probably resulting from the highest amounts of squalene, vitamin D, and vitamin K extracted by SC-CO₂.

The antimicrobial activity of the extracted fish oils was tested against *B. cereus* (gram-positive) and *E. coli* (gram-negative), and the results are shown in Table 8. *E. coli* was highly susceptible to CLO as the MIC and MBC values were the lowest (125 µg/mL and 250 µg/mL, respectively). However, these values doubled for *B. cereus* treated with the oils, with MIC and MBC values reaching 250 µg/mL and 500 µg/mL, respectively. This is a remarkable finding as most antimicrobial agents are unable to act against Gram-negative species due to the complex cell wall structure (Surendhiran, Li, Cui, & Lin, 2021). The high squalene content in cod liver oil might be responsible for the excellent antimicrobial activity against *E. coli*.



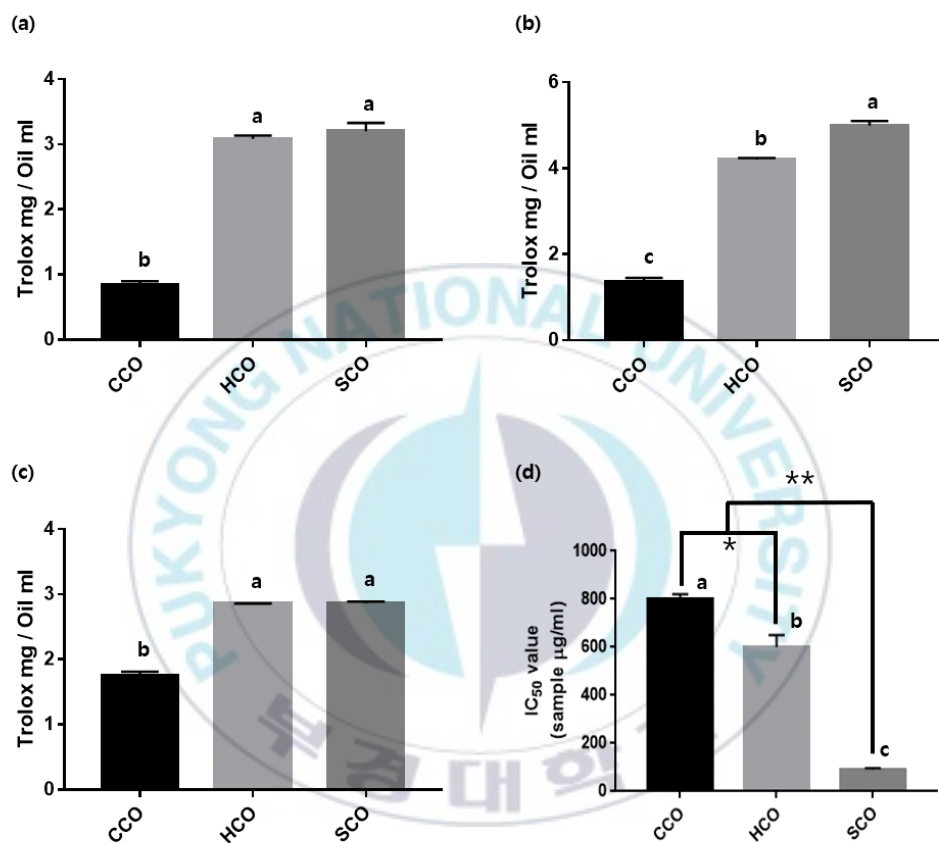


Fig. 7. In-vitro biological activities of oils for antioxidant and cell viability assays (a) DPPH, (b) ABTS⁺, (c) FRAP, (d) AGS cell viability, Different letters indicate significant difference ($p < 0.05$), and at different significance levels, * and ** for $p < 0.05$ and $p < 0.001$ respectively

Table 9. Minimum inhibitory concentration (MIC) and minimum bactericidal concentration (MBC) of cod liver oil against *E. coli* and *B. cereus*

Materials	Bacterium			
	<i>E. coli</i>		<i>B. cereus</i>	
	MIC ($\mu\text{g/mL}$)	MBC ($\mu\text{g/mL}$)	MIC ($\mu\text{g/mL}$)	MBC ($\mu\text{g/mL}$)
CCO	125	250	250	500
HCO	125	250	250	500
SCO	125	250	250	500

3.7 Encapsulation yield and efficiency (EE)

The yield and encapsulation efficiency (EE) of squalene in SLPs generated under different conditions were shown in Table 10. The yield of the produced SLPs ranged from 64.71 ± 0.64 to $71.13 \pm 0.44\%$, showing no significant change in pressure, but we confirmed that the yield changed as the mixing ratio of SCO increased. However, as shown in Table 10, the EE(%) of squalene in SLPs increased significantly with increase in pressure and the mixing ratio of SCO. HPLC analysis of standard squalene, SCO and EE (%) at different pressure changes is shown in Fig. 8. Under the 4:20 mixing ratio of SCO and PEG, EE (%) increased from $14.68\% \pm 0.11\%$, $20.87\% \pm 0.04\%$, and to $35.52\% \pm 0.22\%$ by increasing the pressure from 15 to 20 and 25 MPa, respectively. Moreover, we confirmed that squalene was not detected with 1-PEG and 2-PEG. This due to insufficient squalene content in the generated SLPs (lower than the limit of detection in HPLC system) because SCO and PEG were not well saturated in SC-CO₂ at 15 MPa pressure. Therefore, the most efficient encapsulation of squalene rich oil extracted from cod liver with PEG was achieved at high pressure and high content of SCO. Previous studies showed that fixing the temperature of the mixing chamber at 50°C, does not significantly affect the

yield and EE (%) (Vo, 2018), when SLPs are produced using PGSS and high temperature is problematic for SCO storage as it can decompose the oil.

Table 10. Recovered SLPs yield and squalene encapsulation efficiency on different pressure and mixing ratio conditions

Pressure (MPa)	Mixing ratio (SCO:PEG, w/w)	Yield (%)	EE (%)
15	1:20	64.71±0.64 ^e	ND
	2:20	69.00±0.72 ^c	ND
	4:20	71.79±0.53 ^a	14.68 ± 0.11 ^d
20	1:20	62.05±1.07 ^f	10.94 ± 0.04 ^f
	2:20	70.01±0.16 ^b	11.93 ± 0.20 ^c
	4:20	70.68±0.12 ^a	20.87 ± 0.04 ^b
25	1:20	68.07±0.29 ^d	14.74 ± 0.06 ^d
	2:20	68.18±0.83 ^d	19.92 ± 0.24 ^c
	4:20	71.13±0.44 ^a	35.52 ± 0.22 ^a

Mean ± SD (n=3),

ND (not detected),

Different letters indicate difference (p<0.05) according to Tukey's multiple range test.

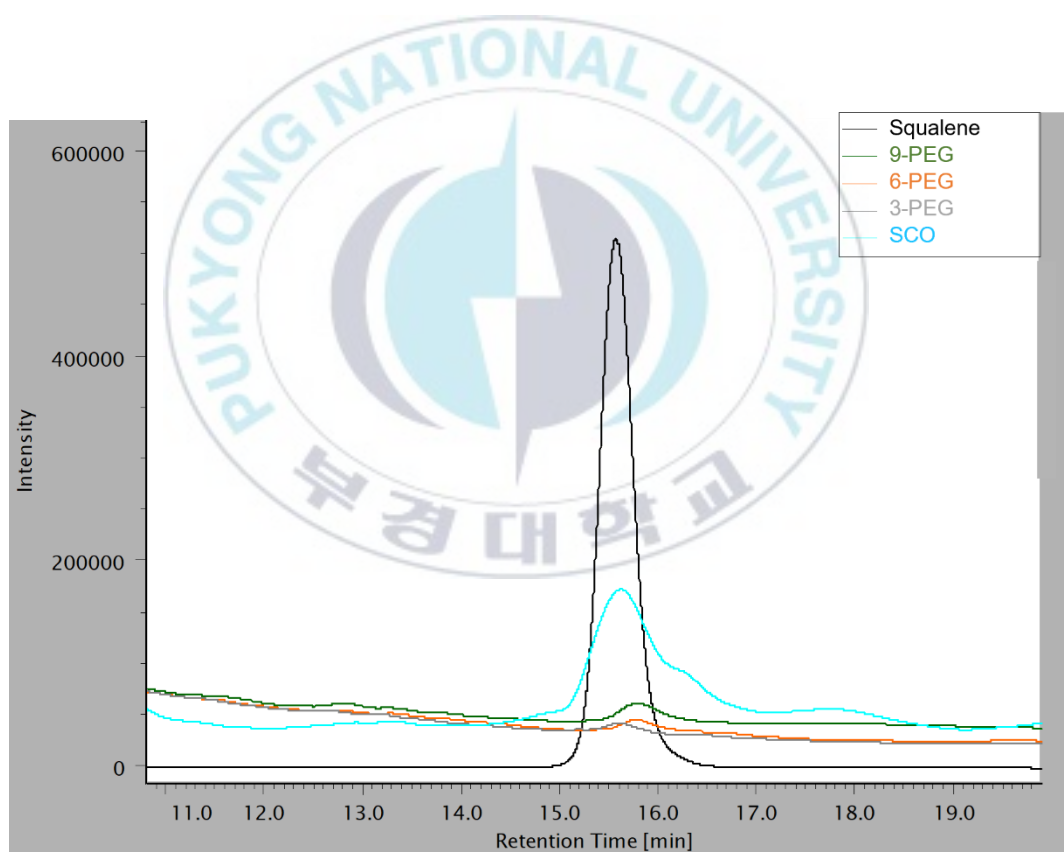


Fig. 8. Squalene contents and encapsulation efficiency chromatogram by HPLC analysis standard; SCO; 3-PEG, 6-PEG; 9-PEG

3.8 Bulk density and tapped density of SLPs and particle size analysis

The bulk density of the powder affects storage, processing, packaging, and distribution of the powder, and the tapped density is useful to describe powder behavior during the powder compaction (Onwulata, 2005). The bulk and tapped density of the SLPs are shown in Table 10. The high bulk density is known to be related to the size of small particles filling the voids between the particles, which reduces the amount of trapped air in the powder. This is important because it reduces the oxidability of the product, and the larger the density, the larger powder can be stored in a smaller container, so the higher the more advantageous in the storage (Carneiro, 2013). As shown in Table 10, the bulk and tapped densities of SLPs obtained under different conditions were from 0.22 ± 0.01 to 0.30 ± 0.02 g/cm³ and from 0.27 ± 0.01 to 0.33 ± 0.02 g/cm³, respectively. The density increased as the pressure increased, showing the highest bulk density of 0.30 ± 0.02 g/cm³ and tapped density of 0.33 ± 0.02 g/cm³ under the mixing condition of 4:20 (SCO:PEG) at 25 MPa. In addition, a high CI value shows a high porosity of the obtained powder, which is known to be related to an irregular shape in particle shape, suggesting that the higher the CI value, the lower the quality of powder. The CI value of the recovered SLPs were shown in a wide range from 24.14

± 1.54 to 9.09 ± 0.97 , and such powder is generally known to exhibit excellent quality of fluidity and cohesiveness when the CI value is 10 or less (Chew, 2018). The CI value was found to be low under the condition of 25 MPa, and the lowest at 9.09 ± 0.97 under the mixed condition of 4:20 (SCO:PEG) of 25 MPa. From the result, 9-PEG was found to be the best in terms of commercial and storage application.

The light scattering analyses showed that all formulations presented a monomodal size distribution profile corresponding to particle size populations. Table 10 showed the $dv(50)$ values decreased to 789.75, 630.89, and 452.54 μm at 15 MPa as the SCO mixing ratio increased, and also decreased to 729.34, 653.25, 426.75 μm at 20 MPa as the SCO mixing ratio increased. And at 25 MPa, it was confirmed that as the SCO mixing ratio increased, the particle size decreased to 493.14, 460.47, and 315.83 μm . This because the size of the particles produced from the PGSS process is a solution saturated with carbon dioxide is rapidly evaporated and expanded in a decompression step small particles are produced (de Paz, 2012). This mean that the size of the particles decreased because the SCO and PEG were well saturated, at a pressure relatively higher than other conditions of 25 MPa, thereby reducing the particle size. In the previous study, as the concentration of lecithin, an emulsifier, increased, the size of the powder produced using PGSS was well saturated with the inner materials and outer wall materials, and the particle size decreased (de Paz, 2012). In the Table 10, the span value means the $D90-D10/D50$ value of the powder, and the smaller span value, the smaller distribution width between particles, and the better quality of the particles. These span values appeared in a wide range from 2.44 to 4.21 and were also the lowest 2.44 at the 9-PEG. In addition, previous studies showed a correlation between the carbon dioxide

saturation concentration of the solution and the particle size of PEG by the PGSS process, indicating that atomization occurs more when the carbon dioxide concentration of the gas saturated solution increases (Varona, 2011). Thus, the degree of saturation of carbon dioxide is effective in producing particles of a smaller size. Therefore, it was found that the 9-PEG from the previous CI value of 9.09 and span value of 2.44 was the best when commercially used.

Table 11. Recovered SLPs density and particle size on different pressure and mixing ratio conditions

Pressure (MPa)	Mixing ratio (SCO:PEG, w/w)	Bulk density (g/cm ³)	Tapped density (g/cm ³)	Carr's index (CI)	Dv(50) μm	span
15	1:20	0.22±0.01 ^c	0.27±0.01 ^b	18.52±1.26 ^c	789.75	4.21
	2:20	0.24±0.01 ^c	0.28±0.01 ^b	14.29±1.24 ^d	630.89	3.18
	4:20	0.24±0.02 ^c	0.31±0.02 ^b	22.58±2.65 ^b	452.54	2.54
20	1:20	0.22±0.01 ^c	0.29±0.01 ^b	24.14±1.54 ^a	729.34	3.63
	2:20	0.24±0.01 ^c	0.29±0.01 ^b	17.24±1.99 ^d	653.25	2.76
	4:20	0.28±0.02 ^b	0.33±0.02 ^a	15.15±1.12 ^d	426.75	2.54
25	1:20	0.25±0.01 ^c	0.29±0.02 ^b	13.79±1.09 ^d	493.14	2.62
	2:20	0.27±0.01 ^b	0.31±0.01 ^b	12.90±1.11 ^c	460.47	2.56
	4:20	0.30±0.02 ^a	0.33±0.02 ^a	9.09±0.97 ^e	315.83	2.44

Mean ± SD (n=3),

Different letters indicate difference ($p < 0.05$) according to Tukey's multiple range test.

3.9 Morphologies of SLPs

The morphologies of the obtained SLPs are shown in Fig. 9, measured the SLPs (a) 3-PEG, (b) 6-PEG, (c) 9-PEG at $\times 150$ magnification, respectively. In (a), it can be seen that the generated particles are in an amorphous state and a lot of agglomeration has been made, also at the (b) can see the amorphous state and agglomeration but, tidier than (a). And in (c), showing the particle size is smaller than that of the other conditions, and a relatively even, generally obtainable form using the PGSS process (Liliana, 2011). The agglomerates observed in the powder is caused by sudden cooling in the PGSS process, and an uncertain spraying force is generated because of sudden cooling in the decompression stage, resulting in binding of small particles (de Paz, 2012). From the Fig. 9, it was confirmed that as the pressure increased, it became more morphologically organized and the particle size decreased. These results are consistent with the previous particle density and size measurement results, and as the pressure increased, the size was relatively even, and small particles were produced.

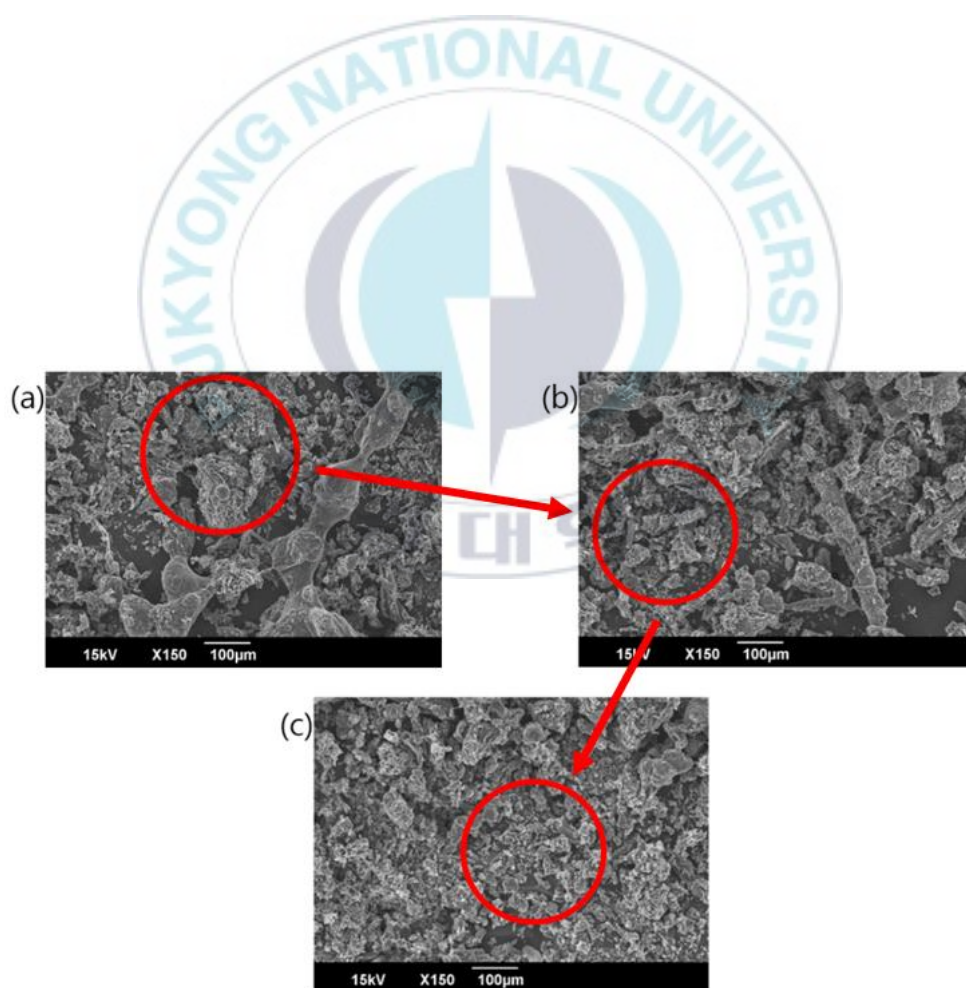


Fig. 9. SEM micro graphs of SLPs recovered from different conditions at magnifications of $\times 150$ (a) 3-PEG, (b) 6-PEG, (c) 9-PEG

3.10 Fourier transform infrared spectroscopy (FTIR)

Evaluation of the presence of squalene in SCO and structural analysis of SLPs before and after encapsulation of SCO were obtained by using FT-IR, and the corresponding results are shown in Fig. 10. In the analysis of the SCO and squalene standards, squalene exhibits antisymmetric vibrations of -CH_3 , -CH_2 at 2962.13 and 2930.31 cm^{-1} , respectively, and asymmetric -CH_2 stretching vibration at 2850.27 cm^{-1} (Petrick, 2009). These absorption bands were detected in SCO with a strong intensity for methylene (-CH_2) groups. The absorption band at 1678.73 cm^{-1} for squalene was associated with a weak -C=C- stretching vibration. The vibration band in the SCO observed at 1751.05 cm^{-1} was associated with a -C=O stretching vibration of the carbonyl groups in SCO. In the region, squalene vibration bands at 1435.74 and 1383.68 cm^{-1} are associated with the -CH_2 scissor and $\text{-C(CH}_3\text{)}$ symmetric bends (Petrick, 2009), which were also detected in the SCO, confirming the presence of squalene. In addition, the structural analysis results of pure PEG 8000 and after encapsulation of SCO with PEG were also shown in Fig. 10. The spectrum bands of pure PEG 8000 were appeared at 2877.27 cm^{-1} -C-H stretching vibrations, and 1479.13 and 1331.60 cm^{-1} -C-H vibrations. . The bands 1280.50 to 1064.51 cm^{-1} were due to

the stretching vibrations of the alcoholic -O-H and -C-O-C ether linkage (Kumar, 2014). After encapsulation, 1751.05 cm^{-1} band, which was not observed in pure PEG, appeared in SLPs, and it was confirmed that -CH₃ and -CH₂ observed in SCO were covered by -CH in pure PEG. From these result, it was confirmed that SCO was well encapsulated in PEG 8000.



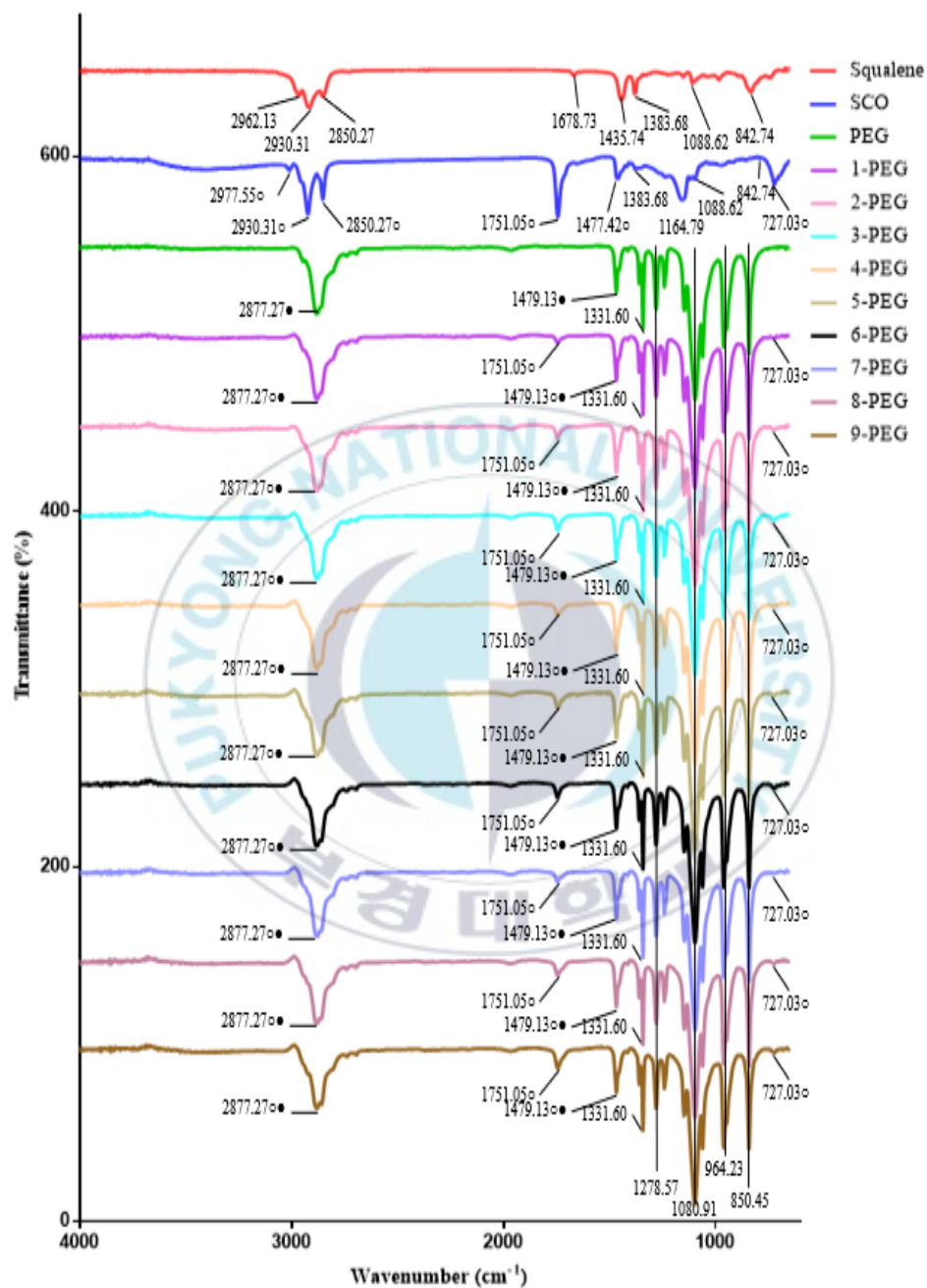


Fig. 10. Fourier transform infrared spectra for squalene, SCO, PEG and SLPs recovered from different conditions (i.e., ○ and ● for SCO and PEG,

respectively)

3.11 X-Ray Diffractometer (XRD) and Differential scanning calorimeter (DSC)

The X-ray diffraction pattern of general pure PEG and the spectrum of SCO encapsulated with PEG 8000 were shown in Fig. 11. The pure PEG 8000 showed strong reflections at 2θ of 19.09° and 23.25° and weak reflections at 14.50° and 26.08° (Corrigan, 2002). The XRD scans shown peak is the intrinsic of crystallinity of pure PEG 8000 and SLPs. The pure PEG 8000 has 185414 counts per second at 19.09° and 190926 counts per second at 23.25° , and the 3-PEG, 6-PEG and 9-PEG were represented at 19.09° 107273, 115945, 124160 counts per second and at 23.25° 119288, 145104, 153422 counts per second. These peaks showed that the main of SLPs were PEG, therefore these give clear evidence for the well encapsulated of SCO in PEG.

DSC analyses were performed to evaluate the physical state of the components of the PEG and SCO, the homogeneity of the final SLPs and the results showed in Fig 12 and Table 11. In the Fig. 12 presents a single endothermic peak. In the previous studies, the pure PEG 8000 is known to represent single endothermic peak (Yam, 2011). The homogeneity of SLPs varied in melting points from 64.02°C to 59.64°C and was the lowest melting point was 59.64°C at the 9-PEG. This reduction of the melting point was shown from the results of the previous EE (%) that the melting point decreases as the encapsulation is done well. Furthermore, from the result in the Fig. 12 the single endothermic peak and in the Table 11 melting point, the SLPs recovered by PGSS process were homogeneous with SCO, without evidence of phase separation or

crystallization. The reduction in magnitude of the XRD peaks in SLPs, together with a reduction in enthalpy change for the melting endotherm by DSC was consistent with some reduction in PEG crystallinity on PGSS process.



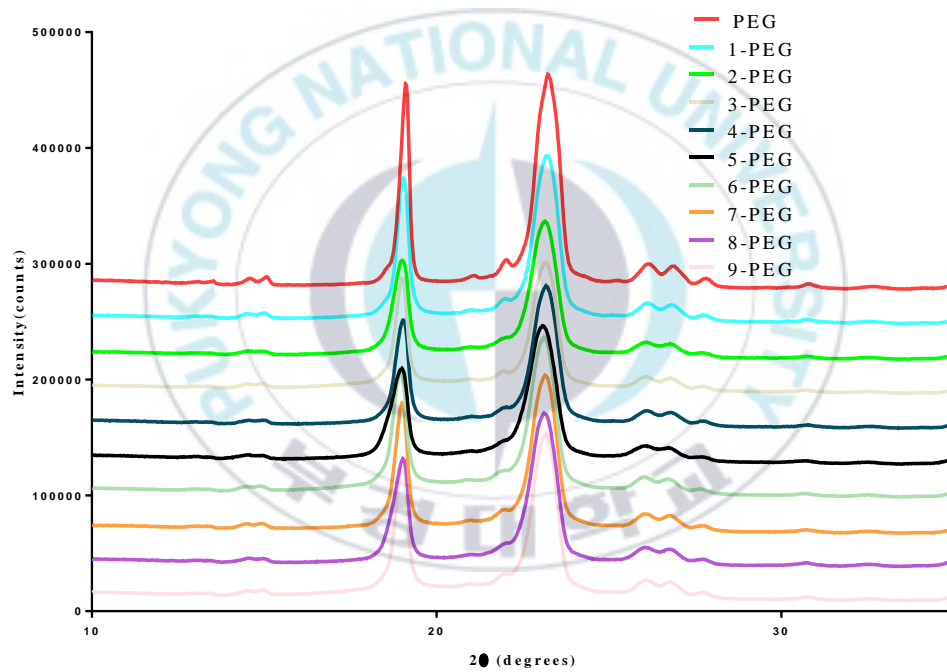


Fig. 11. X-ray diffraction patterns of PEG and SLPs recovered from different conditions

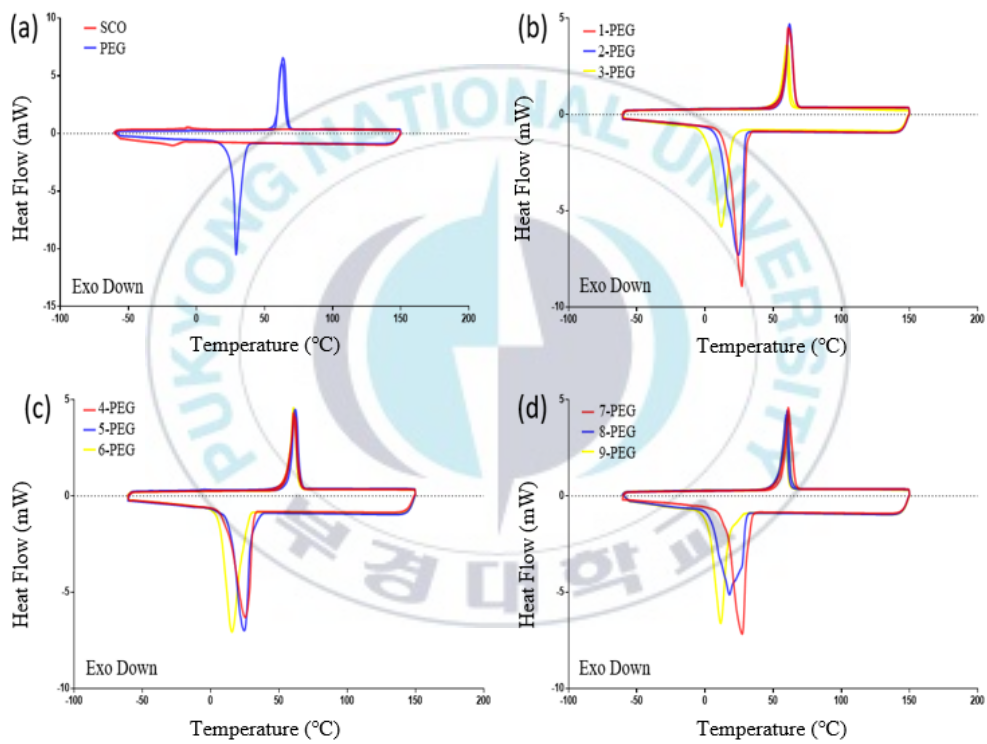


Fig. 12. DSC endothermic and exothermic chromatogram of SCO, PEG and SLPs

Table 12. Recovered SLPs, PEG and SCO crystallization temperature and melting point from DSC analysis

	Crystallization temperature (°C)	Melting point (°C)
SCO	-15.91	-6.85
PEG	29.30	64.02
1-PEG	28.22	61.46
2-PEG	24.76	61.40
3-PEG	13.02	60.98
4-PEG	24.81	62.23
5-PEG	24.65	61.66
6-PEG	14.22	60.84
7-PEG	27.14	61.28
8-PEG	19.21	60.62
9-PEG	12.44	59.64

3.12 Antioxidant activity

The results of measuring the antioxidant activity of SCO and the produced SLPs through ABTS⁺ and DPPH methods were shown in Fig. 13. The antioxidant activity of the ABTS⁺ assay showed that the SCO was 241.67 ± 10.69 mgTE/mL oil, 3-PEG was 99.85 ± 4.17 mgTE/g SLP, 6-PEG was 122.73 ± 5.02 mgTE/g SLP, and 9-PEG was 142.60 ± 5.71 mgTE/g SLP. And the antioxidant activity of the DPPH assay at the SCO was 410.33 ± 3.05 mgTE/mL oil, 3-PEG was 16.49 ± 2.17 mgTE/g SLP, 6-PEG was 23.33 ± 3.06 mgTE/g SLP, and 9-PEG was 30.38 ± 1.44 mgTE/g SLP. In the previous study, it was confirmed that squalene has demonstrated strong *in vivo* antioxidant activities in mice and was suggested to modulate oxidative stress (Ravi Kumar, 2016). Therefore, it was confirmed that antioxidant activity increased as the EE (%) of squalene in SLPs increased. This antioxidant activity was related not only to the contents of squalene, but also to the presence of a carbonyl group, which was observed in SCO after encapsulation from the previous FT-IR results, but not detected in pure PEG 8000, and the presence of a hydroxy group in SLPs after encapsulation. These carbonyl groups and hydroxy groups were known to affect free radical scavenging of antioxidant activity (Tsimogiannis, 2004). Therefore, the results of antioxidant activity using the corresponding ABTS⁺ and DPPH assays indicate that encapsulation was well accomplished as the pressure increases as SCO and PEG saturated, and the squalene, carbonyl groups and hydroxy groups of SLPs, it acts on antioxidant activity, indicating that it was more effective in free radical scavenging.

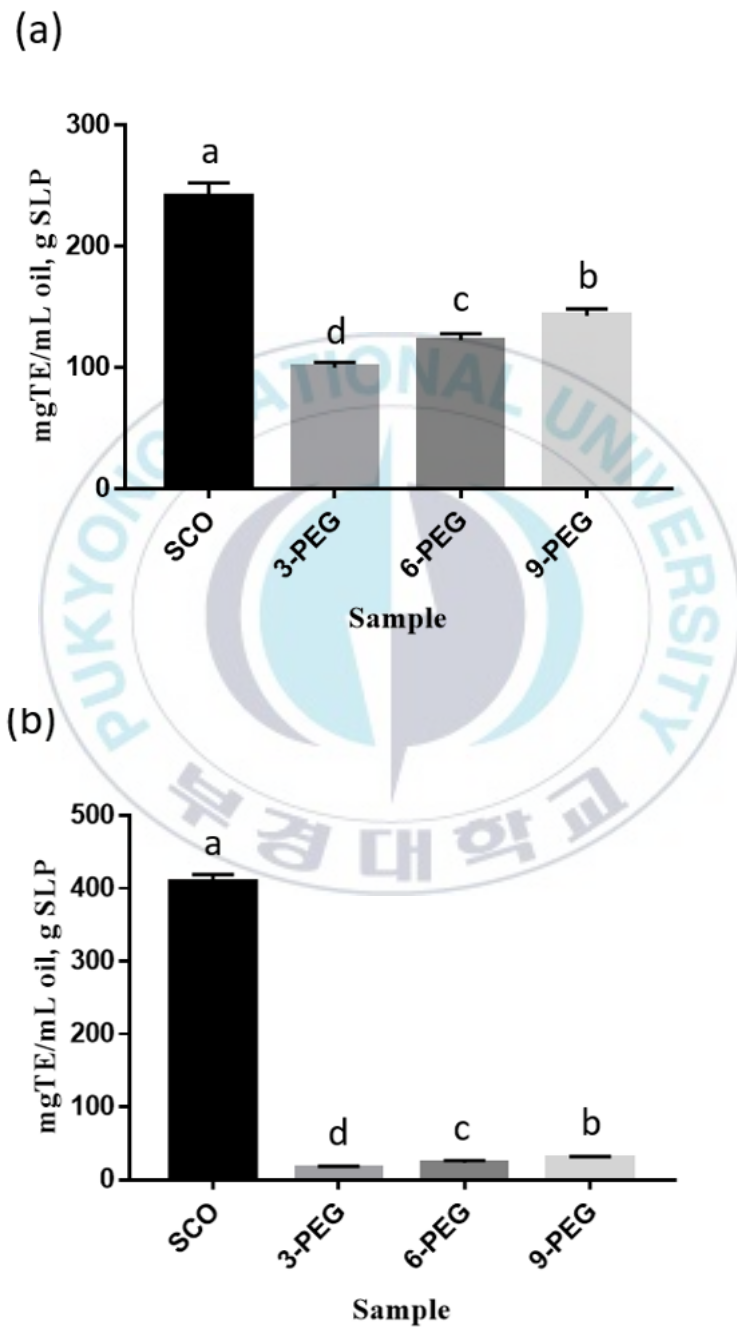


Fig. 13. Antioxidant activity evaluation of SCO and SLPs (a) ABTS⁺, (b) DPPH

3.13 AV and POV value

In order to evaluate the oxidation safety of SCO after encapsulation, the acid value (AV) and peroxide value (POV) of SCO and 9-PEG were measured, and changes in AV and POV due to the oxidation of SCO and 9-PEG were shown in Fig. 14. In the AV result, it was confirmed that SCO was changed from 15.94 ± 0.26 mg KOH/g to 18.45 ± 1.07 mg KOH/g, and 9-PEG was changed from 3.18 ± 0.88 mg KOH/g to 4.40 ± 0.19 mg KOH/g. Although the AV did not show a significant increase over time, the change in POV showed that SCO ranged from 7.46 ± 0.21 meq/kg to 22.50 ± 0.30 meq/kg, 9-PEG ranged from 2.99 ± 0.57 meq/kg to 4.33 ± 0.68 meq/kg. This was due to a significant increase in POV over time in SCO and a delay in the increase in POV after 9 days, whereas the significant increase in POV in 9-PEG where encapsulation was performed was not observed even after time. From this result, it was found that the encapsulated SLP using PEG showed a significant effect on the inhibition of oxidation of SCO.

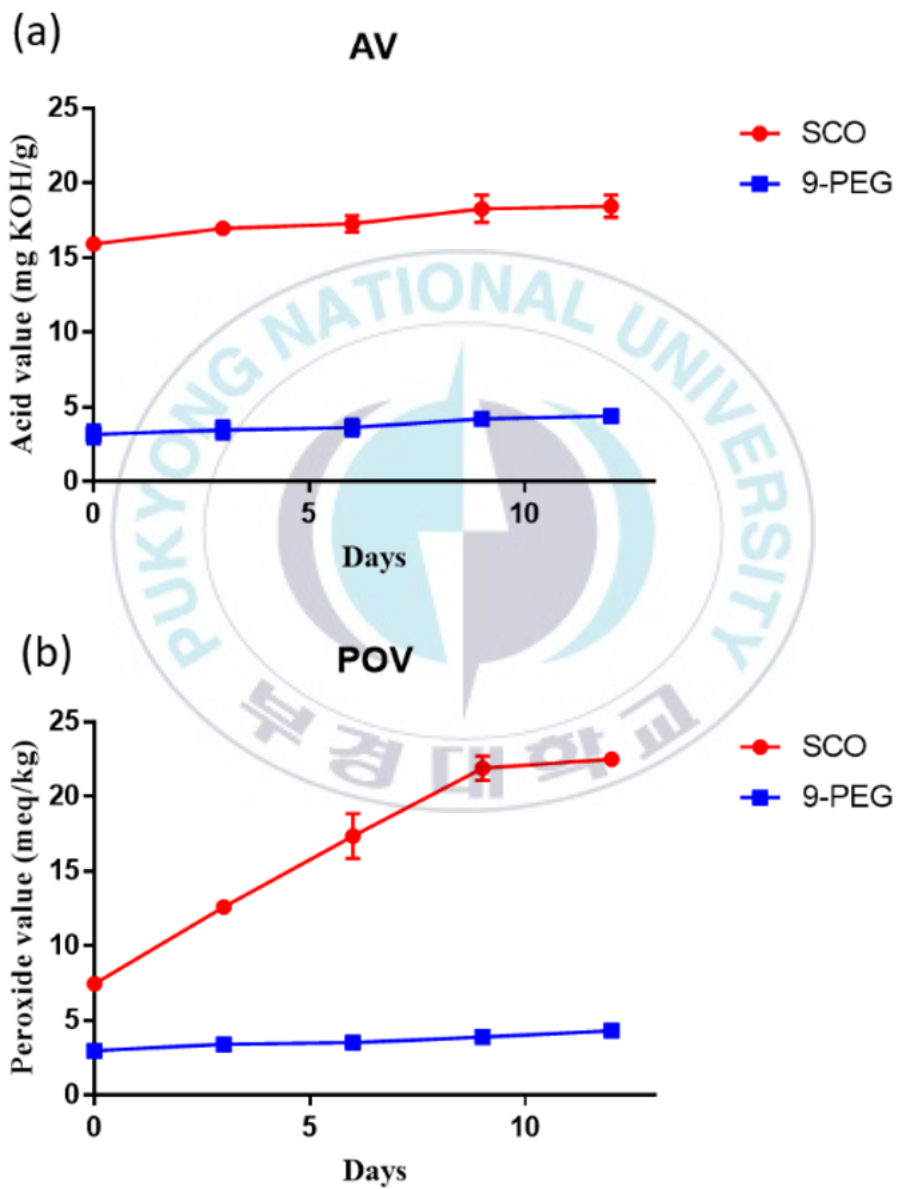


Fig. 14. AV and POV value of SCO and 9-PEG changes on days (a) acid value (b) peroxide value

4. Conclusions

In the present study, cod liver oil was extracted from visceral parts using SC-CO₂, hexane, and pressing extraction methods. Key parameters of SC-CO₂ extraction affecting the oil extractability, i.e., temperature, pressure, and CO₂ flow rate, were optimized using RSM to maximize the extraction yield of oil. The oil obtained by SC-CO₂ extraction exhibited the highest squalene, vitamin D, and vitamin K content and, consequently, showed the best antioxidant and anticancer activities. CLO also had good antimicrobial properties against *E. coli* and *B. cereus*. Moreover, the safety of the oils assessed by analysis of heavy metals revealed that the selectivity of SC-CO₂ for non-polar compounds drastically decreased the amount of toxic heavy metals in the final product. This study demonstrates the potential of SC-CO₂ for recovering functional oils from cod liver viscera. The biological properties and safety of oils obtained by SC-CO₂ extraction indicate that CLO might be a great source of functional ingredients useful in nutraceutical and cosmetic products design.

This study applied downstream process which SC-CO₂ and PGSS process, for extracting functional oil and functional SLPs. As a result of determining the encapsulation yield and EE of SLPs obtained under different conditions from the oil, which produced using SCO, the yield was the highest at 71.13 ±0.44 %, EE 35.52 ±0.22 % at 9-PEG. In addition, the generated SLPs of bulk density and tapped were 0.30 ±0.02 g/cm³, 0.33 ±0.02 g/cm³, respectively, which were also the highest at 9-PEG, and the corresponding Carr's index (CI) value was the lowest 9.09 ±0.97. The particle

size was also the smallest 315.83 nm at 9-PEG. The high bulk density is known to be related to the size of small particles filling the voids between the particles, which reduces the amount of trapped air in the powder, so this is important because it reduces the oxidability of the products, and the larger the density, the larger powder can be stored in a smaller container. The 9-PEG have high density and small particle size, so it has more advantageous in the storage and application in the commercial field. The typical form of powder from PGSS process was confirmed through a scanning electron microscope (SEM), and the presence of squalene in the SCO and the encapsulation of SCO in the produced SLPs were confirmed through Fourier transform infrared spectroscopy (FTIR) analysis. From the X-Ray Diffractometer (XRD) analysis to confirm the crystallinity of the powder and Differential scanning calorimeter (DSC) analysis, the melting point of SLPs were 4.02 °C to 59.64 °C, but at 9-PEG reducing to 59.64 °C. It was confirmed that SCO encapsulation using PGSS process was well achieved. Antioxidant activity evaluation, one of the main physiological activities of squalene, was performed, and the results, 9-PEG with the highest EE(%) was the highest at ABTS⁺ 142.60 ± 5.71 mgTE/g, at DPPH 30.38 ± 1.44 mgTE/g, respectively. After encapsulation, an oxidation stability evaluation of SCO was performed to confirm that the peroxide value of SCO changed to 7.46±0.21 meq/kg to 22.50±0.30 meq/kg, whereas at 9-PEG, it did not show a significant change to 2.99±0.57 mg KOH/g to 4.33±0.68 meq/kg. Therefore, the encapsulation of SCO using PGSS process by PEG 8000 matrix was effective in encapsulation of SCO, and it has advantages for application on commercial fields.

Reference

- S.-K. Kim, F. Karadeniz, Biological importance and applications of squalene and squalane, *Advances in food and nutrition research*, 65 (2012) 223-233.
- S. Senthilkumar, S.K. Yogeeta, R. Subashini, T. Devaki, Attenuation of cyclophosphamide induced toxicity by squalene in experimental rats, *Chemico-Biological Interactions*, 160 (2006) 252-260.
- G. Lippi, G. Targher, M. Franchini, Vaccination, squalene and anti-squalene antibodies: facts or fiction, *European Journal of Internal Medicine*, 21 (2010) 70-73.
- F. Dormont, R. Brusini, C. Cailleau, F. Reynaud, A. Peramo, A. Gendron, J. Mougin, F. Gaudin, M. Varna, P. Couvreur, Squalene-based multidrug nanoparticles for improved mitigation of uncontrolled inflammation in rodents, *Science Advances*, 6 (2020) 23.
- G. Caruso, R. Floris, C. Serangeli, L. Di Paola, Fishery wastes as a yet undiscovered treasure from the sea: Biomolecules sources, extraction methods and valorization, *Marine Drugs*, 18 (2020) 622.
- F. Chemat, M. Abert-Vian, A.S. Fabiano-Tixier, J. Strube, L. Uhlenbrock, V. Gunjevic, G. Cravotto, Green extraction of natural products. Origins, current status, and future challenges, *TrAC Trends in Analytical Chemistry*, 118 (2019) 248-263.

- S. Ahmadkelayeh, K. Hawboldt, Extraction of lipids and astaxanthin from crustacean by-products: A review on supercritical CO₂ extraction, *Trends in Food Science and Technology*, 103 (2020) 94-108.
- S.C.B. Bavisetty, B. Narayan, An improved RP-HPLC method for simultaneous analyses of squalene and cholesterol especially in aquatic foods, *Journal of Food Science and Technology*, 52 (2015) 6083-6089.
- D. Nkurunziza, T.C. Ho, R.A. Protzman, Y.-J. Cho, A.T. Getachew, H.-J. Lee, B.S. Chun, Pressurized hot water crosslinking of gelatin-alginate for the enhancement of spent coffee oil emulsion stability, *The Journal of Supercritical Fluids*, 169 (2021) 105120.
- C. Nasuti, D. Fedeli, L. Bordoni, M. Piangerelli, M. Servili, R. Selvaggini, R. Gabbianelli, Anti-inflammatory, anti-arthritic and anti-nociceptive activities of *Nigella sativa* oil in a rat model of arthritis, *Antioxidants*, 8 (2019) 342.
- M.T. Morales, R. Przybylski, Olive oil oxidation, in: *Handbook of olive oil*, Springer, 2013, pp. 479-522.
- M.S.H. Ruslan, Z. Idham, L. Nian Yian, M.A. Ahmad Zaini, M.A. Che Yunus, Effect of operating conditions on catechin extraction from betel nuts using supercritical CO₂-methanol extraction, *Separation Science and Technology*, 53 (2018) 662-670.
- T.C. Confortin, I. Todero, J.F. Soares, T. Brun, L. Luft, G.A. Ugalde, V. Dal Prá, M.A. Mazutti, G.L. Zabot, M.V. Tres, Extraction and composition of

- extracts obtained from *Lupinus albescens* using supercritical carbon dioxide and compressed liquefied petroleum gas, *The Journal of Supercritical Fluids*, 128 (2017) 395-403.
- Y.-C. Yang, M.-C. Wei, T.-C. Huang, S.-Z. Lee, Extraction of protocatechuic acid from *Scutellaria barbata* D. Don using supercritical carbon dioxide, *The Journal of Supercritical Fluids*, 81 (2013) 55-66.
- J. Ndayishimiye, A.T. Getachew, B.S. Chun, Comparison of characteristics of oils extracted from a mixture of citrus seeds and peels using hexane and supercritical carbon dioxide, *Waste and biomass valorization*, 8 (2017) 1205-1217.
- S. Sathivel, W. Prinyawiwatkul, I.I. Negulescu, J.M. King, B. Basnayake, Thermal degradation of FA and catfish and menhaden oils at different refining steps, *Journal of the American Oil Chemists' Society*, 80 (2003) 1131-1134.
- J. Huang, S. Sathivel, Thermal and rheological properties and the effects of temperature on the viscosity and oxidation rate of unpurified salmon oil, *Journal of food engineering*, 89 (2008) 105-111.
- M. Wesołowski, J. Erecińska, Thermal analysis in quality assessment of rapeseed oils, *Thermochimica acta*, 323 (1998) 137-143.
- L. Petrick, Y. Dubowski, Heterogeneous oxidation of squalene film by ozone under various indoor conditions, *Indoor Air*, 19 (2009) 381-391.

- S. Gunawan, N.S. Kasim, Y.-H. Ju, Separation and purification of squalene from soybean oil deodorizer distillate, *Separation and Purification Technology*, 60 (2008) 128-135.
- M. Castro-González, M. Méndez-Armenta, Heavy metals: Implications associated to fish consumption, *Environmental Toxicology and Pharmacology*, 26 (2008) 263-271.
- M.S. Taleshi, G. Raber, J.S. Edmonds, K.B. Jensen, K.A. Francesconi, Arsenolipids in oil from blue whiting *Micromesistius poutassou*—evidence for arsenic-containing esters, *Scientific Reports*, 4 (2014) 1-7.
- N. Rubio-Rodríguez, M. Sara, S. Beltrán, I. Jaime, M.T. Sanz, J. Rovira, Supercritical fluid extraction of fish oil from fish by-products: A comparison with other extraction methods, *Journal of Food Engineering*, 109 (2012) 238-248.
- A. Al-Gheethi, R. Mohamed, E. Noman, N. Ismail, O.A. Kadir, Removal of heavy metal ions from aqueous solutions using *Bacillus subtilis* biomass pre-treated by supercritical carbon dioxide, *CLEAN—Soil, Air, Water*, 45 (2017).
- P. Kraujalis, P.R. Venskutonis, Supercritical carbon dioxide extraction of squalene and tocopherols from amaranth and assessment of extracts antioxidant activity, *The Journal of Supercritical Fluids*, 80 (2013) 78-85.

- S. Ravi Kumar, B. Narayan, Y. Sawada, M. Hosokawa, K. Miyashita, Combined effect of astaxanthin and squalene on oxidative stress in vivo, *Molecular and Cellular Biochemistry*, 417 (2016) 57-65.
- D. Surendhiran, C. Li, H. Cui, L. Lin, Marine algae as efficacious bioresources housing antimicrobial compounds for preserving foods-A review, *International Journal of Food Microbiology*, 358 (2021) 109416.
- A. León-Buitimea, C.R. Garza-Cárdenas, J.A. Garza-Cervantes, J.A. Lerma-Escalera, J.R. Morones-Ramírez, The demand for new antibiotics: antimicrobial peptides, nanoparticles, and combinatorial therapies as future strategies in antibacterial agent design, *Frontiers in Microbiology*, (2020) 1669.
- S.A. Ashraf, M. Adnan, M. Patel, A.J. Siddiqui, M. Sachidanandan, M. Snoussi, S. Hadi, Fish-based bioactives as potent nutraceuticals: Exploring the therapeutic perspective of sustainable food from the sea, *Marine Drugs*, 18 (2020) 265.
- A.-L. Välimaa, S. Mäkinen, P. Mattila, P. Marnila, A. Pihlanto, M. Mäki, J. Hiidenhovi, Fish and fish side streams are valuable sources of high-value components, *Food Quality and Safety*, 3 (2019) 209-226.
- L. Mondello, P.Q. Tranchida, P. Dugo, G. Dugo, Rapid, micro-scale preparation and very fast gas chromatographic separation of cod liver oil fatty acid

- methyl esters, *Journal of Pharmaceutical and Biomedical Analysis*, 41 (2006) 1566-1570.
- L.L. Gershbein, E.J. Singh, Hydrocarbons of dogfish and cod livers and herring oil, *Journal of the American Oil Chemists' Society*, 46 (1969) 554-557.
- Y.M. Yang, K.Y. Han, B.S. Noh, Analysis of lipid oxidation of soybean oil using the portable electronic nose, *Food Science and Biotechnology*, 9 (2000) 146-150.
- L. Xu, X. Yu, L. Liu, R. Zhang, A novel method for qualitative analysis of edible oil oxidation using an electronic nose, *Food Chemistry*, 202 (2016) 229-235.
- E. Naziri, R. Consonni, M.Z. Tsimidou, Squalene oxidation products: Monitoring the formation, characterisation and pro-oxidant activity, *European Journal of Lipid Science and Technology*, 116 (2014) 1400-1411.
- M. Fraile, D. Deodato, S. Rodriguez-Rojo, I. Nogueira, A. Simplicio, M. Cocero, C. Duarte, Production of new hybrid systems for drug delivery by PGSS (Particles from Gas Saturated Solutions) process, *The Journal of Supercritical Fluids*, 81 (2013) 226-235.
- M.-K. Roh, M. Uddin, B.-S. Chun, Extraction of fucoxanthin and polyphenol from *Undaria pinnatifida* using supercritical carbon dioxide with co-solvent, *Biotechnology and Bioprocess Engineering*, 13 (2008) 724-729.
- T. Rosales-García, J.M. Rosete-Barreto, A. Pimentel-Rodas, G. Davila-Ortiz, L.A. Galicia-Luna, Solubility of squalene and fatty acids in carbon dioxide

- at supercritical conditions: binary and ternary systems, *Journal of Chemical and Engineering Data*, 63 (2018) 69-76.
- S. Šešlija, A. Nešić, J. Ružić, M.K. Krušić, S. Veličković, R. Avolio, G. Santagata, M. Malinconico, Edible blend films of pectin and poly (ethylene glycol): Preparation and physico-chemical evaluation, *Food Hydrocolloids*, 77 (2018) 494-501.
- A. Pestieau, F. Krier, P. Lebrun, A. Brouwers, B. Streel, B. Evrard, Optimization of a PGSS (particles from gas saturated solutions) process for a fenofibrate lipid-based solid dispersion formulation, *International Journal of Pharmaceutics*, 485 (2015) 295-305.
- J. Fages, H. Lochard, J.-J. Letourneau, M. Sauceau, E. Rodier, Particle generation for pharmaceutical applications using supercritical fluid technology, *Powder Technology*, 141 (2004) 219-226.
- B.T. Griffin, M. Kuentz, M. Vertzoni, E.S. Kostewicz, Y. Fei, W. Faisal, C. Stillhart, C.M. O'Driscoll, C. Reppas, J.B. Dressman, Comparison of in vitro tests at various levels of complexity for the prediction of in vivo performance of lipid-based formulations: case studies with fenofibrate, *European Journal of Pharmaceutics and Biopharmaceutics*, 86 (2014) 427-437.

- S. Varona, S. Kareth, Á. Martín, M.J. Cocero, Formulation of lavender essential oil with biopolymers by PGSS for application as biocide in ecological agriculture, *The Journal of Supercritical Fluids*, 54 (2010) 369-377.
- D. Nkurunziza, T.C. Ho, R.A. Protzman, Y.-J. Cho, A.T. Getachew, H.-J. Lee, B.S. Chun, Pressurized hot water crosslinking of gelatin-alginate for the enhancement of spent coffee oil emulsion stability, *The Journal of Supercritical Fluids*, 169 (2021) 105120.
- M. Tun Norbrillinda, H. Mahanom, N. Nur Elyana, S. Nur Intan Farina, Optimization of spray drying process of *Sargassum muticum* color extract, *Drying Technology*, 34 (2016) 1735-1744.
- M. Xie, X. Dong, Y. Yu, L. Cui, A novel method for detection of lipid oxidation in edible oil, *LWT*, 123 (2020) 109068.
- D.T. Vo, P.S. Saravana, H.C. Woo, B.-S. Chun, Fucoxanthin-rich oil encapsulation using biodegradable polyethylene glycol and particles from gas-saturated solutions technique, *Journal of CO₂ Utilization*, 26 (2018) 359-369.
- H.C. Carneiro, R.V. Tonon, C.R. Grosso, M.D. Hubinger, Encapsulation efficiency and oxidative stability of flaxseed oil microencapsulated by spray drying using different combinations of wall materials, *Journal of Food Engineering*, 115 (2013) 443-451.

- S.C. Chew, C.P. Tan, K.L. Nyam, Microencapsulation of refined kenaf (*Hibiscus cannabinus* L.) seed oil by spray drying using β -cyclodextrin/gum arabic/sodium caseinate, *Journal of Food Engineering*, 237 (2018) 78-85.
- E. de Paz, Á. Martín, M.J. Cocero, Formulation of β -carotene with soybean lecithin by PGSS (Particles from Gas Saturated Solutions)-drying, *The Journal of Supercritical Fluids*, 72 (2012) 125-133.
- S. Varona, A. Martín, M.J. Cocero, Liposomal incorporation of lavender essential oil by a thin-film hydration method and by particles from gas-saturated solutions, *Industrial and Engineering Chemistry Research*, 50 (2011) 2088-2097.
- G. Liliana, V. Salima, C.A.M. José, Encapsulation of garlic essential oil by batch PGSS process, *Innovative Romanian Food Biotechnology*, (2011) 60-67.
- E. de Paz, Á. Martín, C.M. Duarte, M.J. Cocero, Formulation of β -carotene with poly-(ϵ -caprolactones) by PGSS process, *Powder Technology*, 217 (2012) 77-83.
- M. Haq, B.S. Chun, Microencapsulation of omega-3 polyunsaturated fatty acids and astaxanthin-rich salmon oil using particles from gas saturated solutions (PGSS) process, *Lwt*, 92 (2018) 523-530.
- L. Petrick, Y. Dubowski, Heterogeneous oxidation of squalene film by ozone under various indoor conditions, *Indoor Air*, 19 (2009) 381-391.

- P. de la Mata, A. Dominguez-Vidal, J.M. Bosque-Sendra, A. Ruiz-Medina, L. Cuadros-Rodríguez, M.J. Ayora-Cañada, Olive oil assessment in edible oil blends by means of ATR-FTIR and chemometrics, *Food Control*, 23 (2012) 449-455.
- P. Kumar, S. Mishra, A. Malik, S. Satya, Preparation and characterization of PEG-Mentha oil nanoparticles for housefly control, *Colloids and Surfaces B: Biointerfaces*, 116 (2014) 707-713.
- D.O. Corrigan, A.M. Healy, O.I. Corrigan, The effect of spray drying solutions of polyethylene glycol (PEG) and lactose/PEG on their physicochemical properties, *International Journal of Pharmaceutics*, 235 (2002) 193-205.
- N. Yam, X. Li, B.R. Jasti, Interactions of topiramate with polyethylene glycol 8000 in solid state with formation of new polymorph, *International Journal of Pharmaceutics*, 411 (2011) 86-91.
- S. Ravi Kumar, B. Narayan, Y. Sawada, M. Hosokawa, K. Miyashita, Combined effect of astaxanthin and squalene on oxidative stress in vivo, *Molecular and Cellular Biochemistry*, 417 (2016) 57-65.
- D. Tsimogiannis, V. Oreopoulou, Free radical scavenging and antioxidant activity of 5, 7, 3', 4'-hydroxy-substituted flavonoids, *Innovative Food Science and Emerging Technologies*, 5 (2004) 523-528.

The logo of Pukyong National University is a circular emblem. It features a central stylized 'P' and 'N' intertwined, with a blue and grey color scheme. The text 'PUKYONG NATIONAL UNIVERSITY' is written in a circular path around the top, and '부경대학교' is written in Korean around the bottom.

Abstract in Korean

초임계 이산화탄소 공정을 이용한 대구 (*Gadus macrocephalus*)
간으로부터 스쿠알렌이 함유된 오일의 추출 및 캡슐화를 통한 산화
안정성 증진

이승찬

부경대학교 대학원 식품공학과

요약

대구의 간유 (CLO)는 기존의 유기용매 및 압착 방법과 친환경 공정인 초임계 이산화탄소 (SC-CO₂) 추출을 이용하여 추출하였다. 온도 (A), 압력 (B), CO₂의 유량 (C)을 추출 주요 매개변수로 설정하여 반응 표면 분석법을 이용하여 수율의 최적화를 실시하였다. 최적 조건에서 추출한 오일의 화학적 조성, 안전성, 열 안정성 및 생리활성 특성을 분석하였다. 초임계 이산화탄소 추출의 최적 조건은 A = 49°C, B = 29.9 MPa, and C = 4.97 mL/min 였다. 그리고 최적 조건에서 오일의 추출은 시간 의존적으로 각각 5, 15, 20 시간 동안 68%, 85%, 89%의 CLO 의 회수율을 보였다. 초임계 추출 오일에서 squalene ($\approx 150 \mu\text{g/mL}$), 비타민 D, K 의 농도가 가장 높고 독성 중금속의 농도가 가장 낮았다. 열중량분석 결과 초임계 추출오일의 열분해 온도가 낮았는데 이는 초임계 추출 오일의 순도가 높기에 이러한 결과가 나타났다. 또한 초임계 추출 대구 간유는 항산화 및 항균 활성에서 높은 활성을 나타냈으며, 영양 산업 및 새로운 기능성 재료 설계에서 잠재적 사용을 시사하는 암세포에 높은 세포독성을 나타냈다. 고체-오일 입자(SLPs)는 청정공정인 PGSS 공정을 이용하여 수득하였으며, 이에 외벽물질로 PEG 를 사용하였다. 입자의 수득 수율 및 캡슐화 효율은 25 MPa, 4:20 (SCO:PEG, w/w), 9-PEG 조건 하에서 각각 $71.13 \pm 0.44\%$, $35.52 \pm 0.22\%$ 였다. 9-PEG 에서 벌크 밀도와 탭 밀도는 각각 $0.30 \pm 0.02 \text{ g/cm}^3$, $0.33 \pm 0.02 \text{ g/cm}^3$, Carr's index 의 값은

9.09±0.97 이었다. 9-PEG 에서 입자 크기는 315.83 nm 였으며, PGSS 공정으로 생성된 분말은 주사 전자 현미경으로 확인하였다. 푸리에 변환 적외선 분광 분석을 통해 CLO 내에 스쿠알렌의 존재와 SLP 에 CLO 의 캡슐화가 이루어진것을 확인하였다. SLP 의 결정성은 X-선 회절계 분석과 시차 주사 열량분석법을 통해 확인되었다. 항산화활성평가에서, 9-PEG 는 각각 ABTS⁺ 에서 142.60±5.71 mgTE/g, DPPH 에서 30.38±1.44 mgTE/g 으로 squalene 의 함량에 따른 높은 항산화활성을 보였다. SLP 의 산화 안정성 평가를 실시하였으며, CLO 의 과산화물가 값은 7.46±0.21 meq/kg 에서 22.50±0.30 meq/kg 으로 급격하게 변화하였으나 SLP 는 유의미한 변화를 보이지 않아 오일의 산화를 유의미하게 억제시켰다.



Acknowledgement in Korean

길지 않던 석사과정동안 과정을 잘 마무리할 수 있도록 도움을 주신 모든 분들께 감사의 인사를 전합니다.

우선 학부생 시절부터 대학원 졸업까지 학문의 길을 나아가는데 있어 끊임없이 조언으로 학문의 길을 이끌어 주시고 무사히 석사 학위를 받게 도와주신 전병수 교수님께 감사의 말씀을 드리고 싶습니다.

그리고 학위를 받는데 있어 심사위원으로 귀중한 시간을 내주어 꼼꼼하게 살펴 주신 안동현 교수님과 심길보 교수님께 진심으로 감사드립니다. 석사과정 동안 학문적 가르침을 주신 양지영 교수님, 이양봉 교수님, 김영목 교수님, 조승목 교수님께도 감사의 마음을 전합니다.

학부생 시절부터 있던 실험실에서 항상 어머니처럼 대해 주시다가 지금은 교수님이 되어 다른 학문적 도움을 주고 계시는 이희정 교수님, 졸업하고 없지만 실험실 생활에 많은 도움을 준 여장부 연진이 누나, 항상 밝았던 유린이 누나, 석사과정 동안 가장 옆에서 든든한 버팀목이 되어준 성렬이 형, 학문적 도움을

많이 준 VIKASH, 언제나 든든한 Truc 실험실 기둥으로 언제나 모두를 돌보아주는 진석이형, 석사 학위과정을 하는데 도움을 많이 준 Surendhiran, 그리고 실험실을 밝게 만들어 주는 지민이, 실험실 들어오자마자 실장 업무 본다고 고생 많은 예슬이, 항상 씩씩한 유나, 가끔 엉뚱한 예련 그리고 부지런한 모습이 보기 좋은 신원이, 다른 외국인 친구들 Amellia, Shiran, David, Bosco, Sadek, Redwan, Akalanka 모든 식품공학실험실 선 후배들에게도 감사의 인사를 전하고 싶습니다.

석사과정을 잘 마칠 수 있도록 격려해준 저의 가족과 친구들에게도 감사의 마음을 전합니다.

비록 저는 졸업을 해서 실험실에서 떠나가지만, 길지 않은 석사과정 동안 많은 것을 배우고 느낄 수 있는 귀중한 경험이었기에 결코 후회가 남지 않는 석사과정 기간 이였습니다.

앞으로 계속해서 실험실을 이끌어 나갈 후배들도 남은 과정을 잘 마무리하여 결코 후회가 남지 않기를 바랍니다.

앞으로 저도 해당 과정동안 얻은 경험을 토대로 앞으로 더욱 성장할 수 있도록 계속 노력하겠습니다. 다시 한번 도움을 주신 모든 분들께 감사의 인사를 전합니다.

감사합니다.